universität wien

MASTERARBEIT / MASTER'S THESIS

Titel der Masterarbeit / Title of the Master's Thesis

„Comparison of *in vitro* plasma stability of *R*-modafinil and its analogue CE-123 in rat and human plasma"

verfasst von / submitted by

Pauline Charlotte Schulze, BSc

angestrebter akademischer Grad / in partial fulfilment of the requirements for the degree of

Magistra pharmaciae (Mag. pharm.)

Wien, 2023 / Vienna, 2023

Studienkennzahl lt. Studienblatt / degree programme code as it appears on the student record sheet:	UA 066 605
Studienrichtung lt. Studienblatt / degree programme as it appears on the student record sheet:	Masterstudium Pharmazie
Betreut von / Supervisor:	Mag. Dr. Judith Wackerlig

Acknowledgements

I would like to thank Mag. Dr. Judith Wackerlig for giving me the opportunity to be part of this research group, supervising my thesis and offering her knowledge whenever needed.

Furthermore, I want to thank Iva Spreitzer, MSc for the co-supervision and the never-ending support and expertise throughout the whole thesis.

Special thanks to Daniel Dobusch, MSc for helping me with all my LC-HRMS measurements.

Finally, I would like to thank all members of the Pharmaceutical Analytics Group for the great time and their support.

Zusammenfassung

R-Modafinil wurde erstmals zur Behandlung von Narkolepsie zugelassen. Mittlerweile gewinnt *R*-Modafinil und das Derivat *S*-CE-123 zunehmende Relevanz zur Verbesserung der kognitiven Leistungsfähigkeit. Anwendung finden sie in der Behandlung diverser Schlafstörungen, Alzheimersymptomen aber auch Rauschgiftabhängigkeit. *S*-CE-123 zeigt eine niedrigere Affinität und höhere Selektivität zu Dopamintransportern als sein Vorgänger und verursacht daher seltener unerwünschte neurologische Arzneimittelwirkungen. Präklinische Plasmastabilitätsstudien weisen auf die Tauglichkeit einer neuen Substanz für folgende klinische Studien hin. Diese Studie ist die Erste, welche die *in vitro* Plasmastabilität von *R*-Modafinil und *S*-CE-123 in Ratten- und Humanplasma verglichen hat. Hierfür wurden Plasmaproben bei 37 °C für 8 h inkubiert und mittels LC-HRMS quantifiziert. In Rattenplasma blieben 6.6±0.5% *R*-Modafinil übrig and 78.3±2.2% wurden in Modafinilsäure metabolisiert. In Humanplasma konnte kein Abbau von *R*-Modafinil festgestellt werden. Die *S*-CE-123-Inkubation ergab keine signifikante Metabolisierung in Ratten- bzw. Humanplasma. Die analytische Methode wurde mittels ICH Guidelines M10 für bioanalytische Methoden (2019) erfolgreich validiert. Die Präzision zwischen Läufen und Richtigkeit waren für 100-4000 ng/mL *R*-Modafinil, 200-3000 ng/mL Modafinilsäure und 100-1500 ng/mL *S*-CE-123 akzeptabel. Weiters wurde die Enzyminhibierungskapazität von 10% DMF und 0,25% NaF getestet. 66.8±7.2% *R*-Modafinil verblieb in DMF-gespiktem und 53.5±4.2% in NaF-gespiktem Plasma nach 6 Stunden. Der $logP_{ow}$-Wert für *R*-Modafinil (0.989±0.018) und *S*-CE-123 (1.57±0.064) wurde mittels HPLC bestimmt und mit den entsprechenden theoretischen Werten von ACD/ChemSketch (1.17±0.49 bzw. 1.81±0.50) verglichen. Die Ergebnisse der *in vitro* Plasmastabilitäts- und $logP_{ow}$ - Experimente zeigen eine Überlegenheit von *S*-CE-123 gegenüber dem zugelassenen *R*-Modafinil.

Abstract

R-modafinil was first approved for the treatment of narcolepsy. Nowadays, *R*-modafinil and its analogue *S*-CE-123 gain increasing relevance as cognitive enhancers to treat sleep disorders, Alzheimer symptoms or even drug addiction. *S*-CE-123 succeeds its parent compound by lower affinity and higher selectivity to dopamine transporters and thus shows fewer neurological adverse effects. Preclinical plasma stability studies are an indicator whether novel drugs are worth going through to the clinical stage. This study is the first in focusing on the *in vitro* plasma stability of *R*-modafinil and *S*-CE-123 in rat and human plasma. Samples were incubated at 37 °C for 8 h and quantified by LC-HRMS. In rat plasma, 6.6±0.5% of *R*-modafinil remained and 78.3±2.2% metabolised to modafinil acid. No *R*-modafinil degeneration was detected in human plasma. There was no significant degradation of *S*-CE-123 in rat nor human plasma detected. Method validation was conducted successfully according to the ICH Guidelines M10 for bioanalytical methods (2019). Between-run precision and accuracy were found acceptable for 100-4000 ng/mL *R*-modafinil, 200-3000 ng/mL modafinil acid and 100-1500 ng/mL *S*-CE-123. Additionally, the enzyme inhibiting capacity of 10% DMF and 0.25% NaF were tested in rat plasma. 66.8±7.2% *R*-modafinil remained in DMF-spiked and 53.5±4.2% in NaF-spiked plasma after 6 h. $LogP_{ow}$ for *R*-modafinil (0.989±0.018) and *S*-CE-123 (1.57±0.064) was detected by HPLC and compared to theoretical values by ACD/ChemSketch (1.17±0.49 and 1.81±0.50, respectively). The *in vitro* plasma stability and $logP_{ow}$ results demonstrated the superiority of *S*-CE-123 over approved *R*-modafinil.

Table of Content

1. Introduction

1.1. *R*-modafinil

Modafinil (2-[(RS)-(diphenylmethyl)sulfinyl]acetamide, *R*-MO,
Figure 1) is a racemic substance which was first introduced for the treatment of excessive somnolence associated with narcolepsy in France in 1994 [1], [2]. Excessive somnolence is defined as having difficulties at staying awake as well as an increased tendency to suddenly fall asleep [3]. Typical treatments for narcolepsy were amphetamines, methylphenidates or suppressing substances like tricyclic antidepressants. Back then, there was an urge for more effective substances than the traditionally used central nervous system (CNS) stimulants [4]. The mentioned CNS stimulants could not fully control the symptoms and had various adverse effects on the central nervous system, the cardiovascular and gastrointestinal system additionally to their high abuse potential [5].

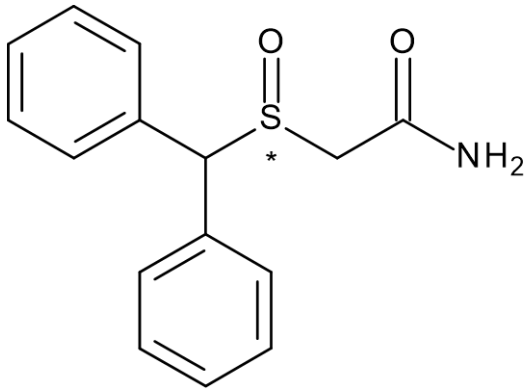

Figure 1. Structure of modafinil. * denotes the chiral centre.

Additionally, to the mentioned purpose, modafinil got approved by the United States Food and Drug Administration (FDA) for treating daytime sleepiness in shift work sleep disorder and obstructive sleep apnoea. It does not affect normal sleep and has beneficial effects on memory and influences on test subject's psychology and behaviour [2], [4]. The antagonising effect of modafinil - through dopamine (DA) transporter inhibition - after cocaine administration, proposes potential treatment for stimulant abuse [6] .

Darwish *et al.* (2009) showed that the maximum plasma concentration C_{max} is reached approximately 2 hours after oral administration on an empty stomach, the steady state within 7 days while under a once-daily administration [7].
The substance's chiral centre at the sulfoxide group (Figure 1) leads to different pharmacological properties of the enantiomers. The racemate's elimination half-life ($t^1/_2$) tends to be around 15 hours after administration which is due to the longer lasting *R*-enantiomer ($t^1/_2$ ≈ 15 hours), also known as armodafinil. The $t^1/_2$ of *S*-modafinil is approximately 4 hours [7]. Although in mice no significant potency difference between the two enantiomers was observed [8], armodafinil is also approved in the United States as individual drug due to its enduring effects. To this date, only two preparations of racemic modafinil are available in Austria [9].

Whereas modafinil is mainly metabolised in the liver, 10% leave the body unchanged *via* renal excretion [8]. Due to the amide group both enantiomers are highly susceptible to hydrolysation *via* esterases and amidases to modafinil acid (MA) (Figure 2 – A) which is then further excreted renally. It is still unclear which of the two enzymes is mainly responsible for the degradation of modafinil as the activity of esterase and amidases could overlap [10]. Wong *et al.* (1999) found that 35-60% of the dose was detected in the urine as MA [4].The other metabolisation way is the sulfone formation (Figure 2 – B) by CYP3A4 and CYP3A5 which belong to the cytochrome P450 enzyme family [11]. Neither of the two metabolites shows any pharmacological effect [8]. After studying the interaction profile of armodafinil with drugs metabolised by specific CYP enzymes, Darwish *et al.* (2008) concluded that armodafinil has no effect on CYP1A2, however, is a moderate CYP3A4 inducer and CYP2C19 inhibitor in healthy subjects. Dosage adjustments for their substrates may be required to reduce the risk of drug-drug interactions [12].

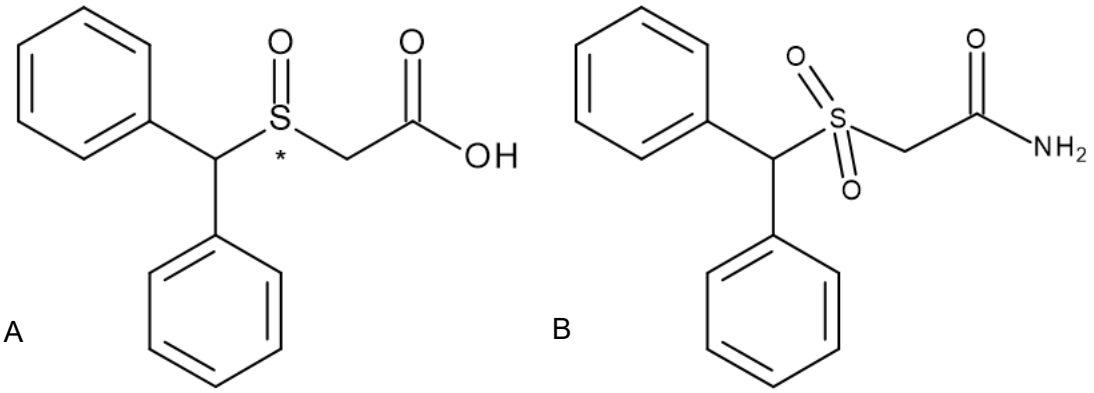

Figure 2. Modafinil acid (A) and modafinil sulfone (B). * denotes the chiral centre.

Modafinil is administered orally as it is basically insoluble in water and only very little in ethanol [13]. In Austria it is approved for narcolepsy with or without cataplexy with 200 mg daily at the beginning with the possibility to increase the dose up to 400 mg per day [3]. Wong *et al.* (1999) looked at daily doses from 200 mg up to 800 mg. However, they had to stop the 800 mg panel after three days due to increased pulse rate and blood pressure. They suggested that 600 mg might be the maximum tolerated daily dose [14].
According to published information by the producer, long-term usage (> 9 weeks) of modafinil should be revaluated on a regular basis. Due to elimination processes of the drug patients with severe hepatic insufficiency should only get half of the usual dose. Furthermore, modafinil dosage should be carefully set in patients with renal insufficiency as there is only insufficient data [3].

In general, armodafinil is well tolerated, mild side effects including headaches, nausea, dizziness, dry mouth, nervousness have shown to be dose dependent [15]. More severe side effects like vasodilation, dose-depended increase of alkaline phosphatase and gamma-glutamyl-transferase, chest pain, tachycardia and palpitations have been documented in at least one in 100 patients. Especially between one and five weeks after therapy start, sever rashes, including Stevens-Johnson-Syndrome, are possibly and require an immediate therapy stop. Modafinil is contraindicated in pregnancy, while breast-feeding and in patients with uncontrolled moderately sever to sever hypertension and arrythmia [3]. Even though, modafinil is in general well tolerated, the urge for more potent and stable, and thus longer lasting, analogues was given [16].

1.2. Modafinil analogues

In process of finding a new lead several molecules were synthesised [16]. This study focused on comparing the plasma stabilities of *S*-CE-123 and *R*-MO, whereas another stable modafinil analogue (CE-137) was used as internal standard in LC-HRMS measurements.

1.2.1. CE-123

The analogue (S)-5-(benzhydrylsulfinylmethyl)-1,3-thiazole or CE-123 (Figure 3) was one of the most promising analogues synthesised. The carboxyl-amid group is substituted by a thiazole ring which is suggested to decrease the vulnerability against esterases and amidases compared to modafinil.

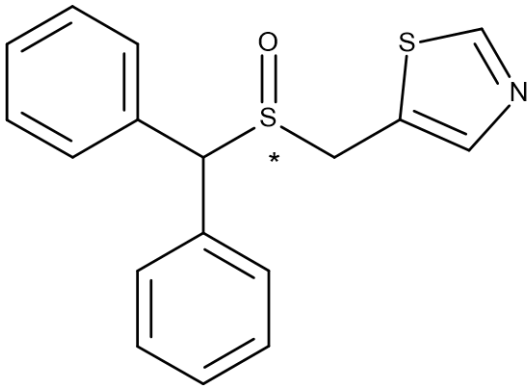

Figure 3. Structure of CE-123. * denotes the chiral centre.

S-CE-123, like its parent compound, causes an increase of expression levels of some hippocampal DA receptors (D1 and D5) and inhibition of DA transporters. Its cognitive enhancing (CE) properties were examined in various studies. Kristofova *et al*. (2018) has shown its beneficial effects on memory acquisition from day one, when treating Sparague-Dawley rats with 1 and 10 mg/kg of the drug. Like for other psychostimulants including modafinil, a dose-dependent effect was observed. From day two onwards cognitive enhancing effects were noted with 1 mg/kg [17].

Studies observed its lower affinity and increased selectivity to inhibiting DA transporters compared to modafinil [17]–[19]. Whereas the *R*-enantiomer of modafinil has been proven to be more active, the *in vitro* activity of *S*-CE-123 is nearly 8 times higher than of *R*-CE-123. All mentioned improvements result in the administration of lower doses and potentially fewer side effects compared to modafinil [20].
Furthermore, Nikiforuk *et al*. 2017 recognised that CE-123 treated rats showed decreased impulsivity than modafinil treated rats, another advantage of the analogue over the parent compound [21].

Further derivatisation of *S*-CE-123 were done by the substitution of a bromide in para-position of one of the phenyl rings. Even though, the inhibition concentration (IC_{50}) was approximately a sixth of its parent compound, toxicity studies showed its unsuitability for *in vivo* studies [20].

1.2.2. CE-137

CE-137 (5-(benzhydrylsulfinylmethyl)-2-methyl-1,3-thiazole) is another analogue of modafinil and structurally similar to CE-123 with an additional methyl group at the thiazole ring (Figure 4) [20].

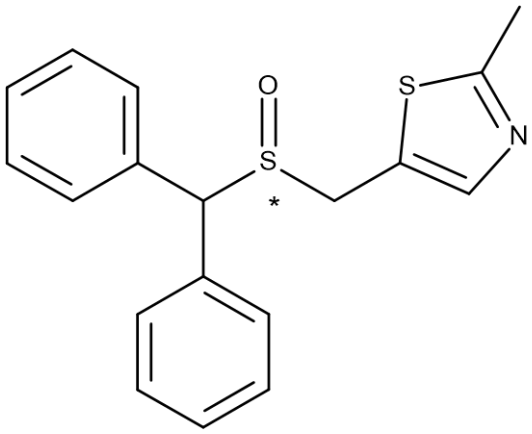

Figure 4. Structure of CE-137, used as internal standard throughout this study. * denotes the chiral centre.

In this study it was used as internal standard for determining the concentration of *R*-MOand *S*-CE-123, due to its structural similarity and its high stability. Kalaba *et al.* (2020) did an *in vitro* study with CE-137 and found that the addition of the methyl group to the thiazole ring resulted in greatly decreased activity on DAT compared to *S*-CE-123 and *R*-MO [20].

1.3. Plasma stability of drugs

Drug stability in plasma is an important characteristic for the success of medical treatments. Plasma metabolisation influences the termination half-life, pharmacokinetic profile and at larger scale hinders reaching sufficient concentration of the drug at the target. Whereas most drugs are metabolised in the liver *via* members of the CYP 450 family and esterases, drugs containing esters, amides, carbamates, phosphates, lactones, lactams, sulfates, sulfonamides and peptides are susceptible for hydrolysation by plasma enzymes. The degradation rate depends on the functional group - esters are hydrolysed more rapidly than amides and sulfonamides, which in turn hydrolyse faster than carbamates [22].
To overcome plasma stability problems *in vivo* it is easiest to exchange the more susceptible targets against less vulnerable groups as it can be seen when comparing the structures of Modafinil and *S*-CE-123 (compare Figure 1 and Figure 3) [16].

Furthermore, biological matrices contain proteins and lipids, which show additional opportunities for non-covalent binding [23]. Plasma protein binding has shown significant influence on the plasma stability of drugs, as it transports the drug to its target while not being fully accessible to plasma esterase hydrolysation. Moreover, protein bound molecules cannot undergo glomerular filtration [24], [25]. In terms of binding small molecules albumin is the most prominent, followed by *α*-1-acid glycoprotein (AAG), globulins and lipoproteins [26]. Albumin binds especially to acidic and neutral drugs [22], [23]. Modafinil shows an approximate plasma protein binding of 60% [3] and additionally a larger distribution volume than total body water (0.624 L/kg) - implicating that it also binds to tissue [4].

Due to differences in enzyme activity and occurrence, the drug stability also depends on species, gender and in humans even ethnicity [4], [10], [27]. Hale *et al.* (2000) showed that hydrolysis rates are higher in rodents than in dogs and even lower in humans [27]. Gender differences in the modafinil metabolism were noted by Wong *et al.* (1999) in a single-dose pharmacokinetic study. It was found that the plasma clearance in young females was significantly higher than in young males with values of 0.88 and 0.72 mL/min/kg, respectively. Thus, they concluded that plasma half-life is shorter in females than in young and elderly males [4]. Wu *et al.* (2012) investigated the influence of ethnicity on the metabolism of modafinil in five different Asian populations - Han, Korean, Uygur, Hui and Mongolian. They noticed increases of modafinil clearance up to 1.25-fold in comparison to the Han group [10]. Due to their results within the studied all-Asian population it can be presumed that the differences between Asians, Africans and Caucasians may be even more significant.
All the previously described studies focused on *in vivo* administration. An obvious disadvantage of *in vitro* drug instability in plasma is noted in therapeutic drug monitoring or forensic examination. It is unusual for samples to be measured immediately after being taken, so a way must be found to stabilise not only the blood/plasma but also protect the drug of interest against degradation [28].

Several papers mentioned the enzyme inhibiting effects of sodium fluoride (NaF) [22], [28]–[31]. Papoutsis *et al*. (2014) investigated to effects of storage temperature and sampling tubes, anticoagulants (ethyl diamine tetra acetic acid (EDTA) and oxalate) and preservative (NaF) on the plasma stability of morphine, codeine and 6-acetylmorphin. All three are identified in blood samples of heroin addicts. Morphine and codeine are also used as individual drugs but 6-acetylmorphin is clear evidence for heroin use. All three of them showed an increased stability in the presence of NaF due to its enzyme inhibiting effect, whereas the type of anticoagulant was not found to have an effect [28].

Di *et al.* (2005) investigated the effects of dimethyl sulfoxide (DMSO) on the plasma stability of various drugs. They found that in general, the higher the DMSO concentration was the more drug was recovered after three hours incubation time. Two of the studied drugs showed an opposite effect, as their recovery rate decreased with increasing DMSO concentration. They concluded that DMSO also interferes with the plasma protein binding and so with a natural protective feature against drug degradation [32].

Another option is 10% dimethylformamide (DMF) as mentioned by Gorman (2002) [33]. This has been successfully tested on modafinil by Sesinova (2020), even though the method is yet to be validated [34].

1.4. Lipophilicity and logP

The lipophilicity is an early measured parameter in drug discovery to assess *in vivo* pharmacokinetics and pharmacodynamics [35], [36]. It allows predictions in terms of plasma protein binding, drug distribution and excretion as well as potential passage of the blood brain barrier (BBB). The latter is especially important for drugs with desired central activity like *R*-MO and *S*-CE-123. Suggested log P_{ow} thresholds for BBB diffusion differ significantly between publications. In general, the evaluation follows the adapted ‘Lipinski’s rule of five’ (Ro5), which states that a log P_{ow} range of 2.0-3.5 indicates for passive diffusion into the brain *via* BBB [36].

Log P_{ow} describes the partition-coefficient of unionised compounds in two non-miscible solvents (e.g. n-octanol and buffer). There are plenty of different methods to determine log P_{ow}

of a substance, although the measured values are not comparable if not measured with the same method. Databases for each method are not available yet. The momentarily 'gold standard' is the shake tube/flask with 1-octanol and phosphate buffered saline (pH 7.4) - logP_{ow}[36]. However, it is limited to a smaller log P_{ow} range than HPLC methods (2-4 instead of 2-6), by interactions of impurities in the compound, low throughput due to long shake times (3-24 h), pK_A differences and the detection limit of 1-octanol with highly hydrophilic substances. HPLC methods also surpass the gold standard in simplicity, speed, lack of impurity interactions and the direct partitioning [36], [37].

1.5. Mass spectrometry

The information about the theory of mass spectrometry of this chapter was taken from Kazakevich's 'HPLC for pharmaceutical scientists' (2007) [38].
In this study a combination of ultra high performance liquid chromatography (UHPLC) and high resolution mass spectrometer (HRMS) was used to quantify the analytes in incubated plasma samples. The MS shows increased sensitivity and isotopic specificity in comparison to an UV detector. These features are crucial when separating *R*-MO and its metabolite MA, as the two are not easily separated by UHPLC due to the similar hydrophily and structure and consequently the elution shortly after each other. MS separates ion mixtures based on mass-to-charge ratios (*m/z)*, offers the analyte molecular mass as well as structural information of fragment ions. Figure 5 shows the schematic set up used.

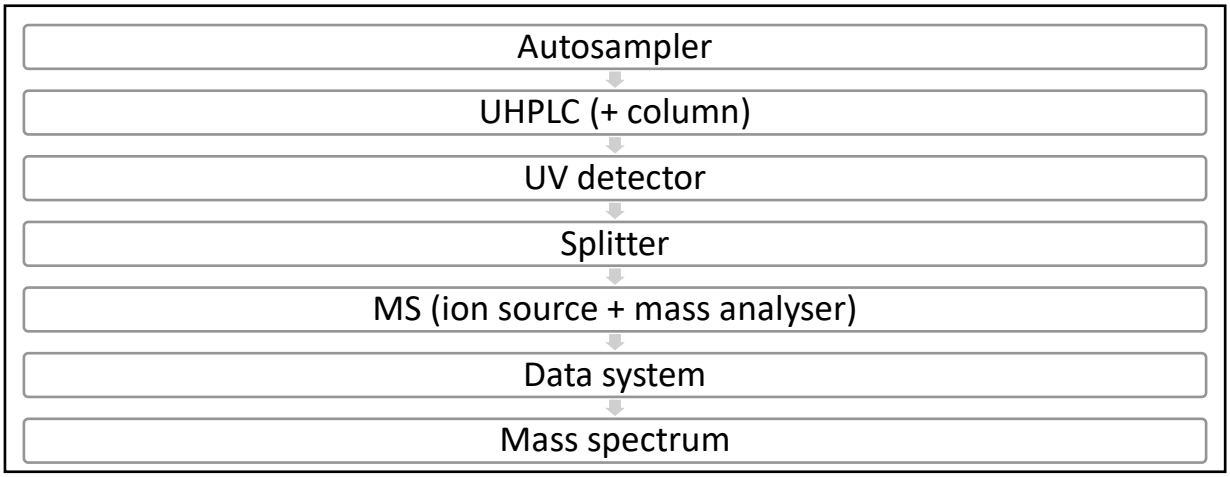

Figure 5. Schematic diagram of the used UHPLC-MS set-up.

1.5.1. MS – ion source

There are two important components of MS, the ion source and mass analyser. The ion source must provide a high ion stability and ionisation efficiency to ensure correct mass analysation by the subsequent mass analyser. Due to the upstream UHPLC the ionisation technique should work at atmospheric pressure. This study used the electrospray ionisation (ESI). It causes the formation of multiply charged ions to a mass accuracy of 0.01%. Additionally, it is a soft ionisation method producing predominantly molecular ions with minimal fragmentation.

After the UV detector the sample runs through a splitter to decrease the flow rate to approximately 200 µL/min to ensure stable spray without change in analyte concentration. In the nebuliser it is mixed with nitrogen (N_2) and sprayed through a charged needle (4-5 kV) into the spray chamber, forming small droplets. By leading preheated N_2 into the spray chamber the solvent evaporates and the droplets shrinkage causing an increase in charge within.

When the force of Coulomb repulsion surpasses the surface tension, the droplets fission to even smaller ones which shrink further due to evaporation. Once the electrical field force at the droplet surface surpasses the surface tension again, ions are released into the gas phase. Depending on the used mode these ions can either be positively or negatively charged.
The ions are lead through a glass capillary to a skimmer and further to the mass analyser.

The positive ion mode, usually used for basic analytes, forms protonated molecular ions $[M+H]^+$ or adducts with Na^+, K^+ or NH_4^+. For acidic analytes usually the negative ion mode is used, which forms either deprotonated molecular ions $[M-H]^-$ or adducts with $CHOO^-$, CH_3COO^- or Cl^-. This study used the positive ion mode.

1.5.2. MS – mass analyser

The mass analyser is responsible to measure mass-to-charge ratios by separating the ions. For measurements where the desired *m/z* ratio is known, the mass analyser can be set to the specific value. However, drug stability studies require the ability to detect multiple unknown *m/z* ratios as degradation processes could lead to various fragments of the parent compound. In this case, the combination of different mass analysers allows to screen for individual ions within a mixture. For this study a quadrupole - quadrupole - time-of-flight (QQ-TOF) combination was used. The fist quadrupole selects the parent ion, which dissociates to product ions in the second quadropoly, which in turn are analysed by the last mass analyser. The dissociation is achieved by letting the ions collide with a collision gas (e.g. Ar or N_2) within the mass spectrometer. This process is called collision-induced dissociation (CID). Another option would be the collision with a surface (SID).

The quadrupole is set up of four parallel rods to which sweeping RF and DC voltages are applied. The DC/RF voltage ratio influences the mass resolution. The quadrupole selects specific ions whereas lighter or heavier ions are evicted from the rod assembly.

A time-of-flight mass spectrometer accelerates the generated ions through known potential and measures their time needed traveling through a flight tube to a detector. The needed travel time is proportional to the *m/z* values of the ions. Lighter ions reach the detector earlier, heavier ions later. As the initial kinetic energy also influences the travel time, the TOF has a reflectron to compensate for these differences. Ions with higher energy penetrate further into the reflectron field and therefore have a longer flight path back to the detector than less energetic ions. The main advantage to scanning mass analyser (e.g. TOF) is the ability to detect all ions almost simultaneously due to a high resolution time counting device.

1.6. Research aim

The in-drug development frequently done *in vitro* microsomal or *in vivo* studies cannot comprehend the plasma enzyme activity as some hydrolysing enzymes are only found in plasma [22]. The aim of this study is to gain a more detailed insight into the plasma stability of *R*-MO, CE-123 and to draw up plasma curves of these two drugs and the metabolite MA. Additionally, two enzyme inhibiting chemicals were to be tested on their inhibition efficacy and so slowing down the degradation process of the drugs of interest.

Furthermore, the plasma stability of both substances was to be compared in rat and human plasma to see if there are significant differences in enzyme activity between these two species and the effect on *R*-MO and CE-123.

2. Methods and Materials

2.1. Chemicals

R-MO, MA, *S*-CE-123 and CE-137 were synthesised by Dr. Predrag Kalaba at the Department of Pharmaceutical Chemistry of the University of Vienna. The following chemicals were purchased: LiChrosolv® acetonitrile (ACN, LC-MS grade) from Merck KGaA (Darmstadt, Germany), water with LC-MS grade from VWR International (Pennsylvania, US), HiPerSolv Chromanorm® Ultra Plus methanol (MeOH, LC-MS grade) from VWR International (Pennsylvania, US), phosphoric acid for analysis (ACS reagent, 85+%) from Acros Organics™ (Massachusetts, US, formic acid (FA, 98+%) from Carl Roth GmbH + Co. KG (Karlsruhe, Germany), LiChrosolv® methanol with HPLC grade from Merck KGaA (Darmstadt, Germany), water with HPLC grade from Carl Roth GmbH + Co. KG (Karlsruhe, Germany), Rotisolv® ACN with HPLC grade from Carl Roth GmbH + Co. KG (Karlsruhe, Germany), Chromasolv™ toluene from Honeywell Riedel-de-Haën (Seelze, Germany), sodiumhydroxid (NaOH) from Merk KGaA (Darmstadt, Germany), disodium hydrogen phosphate anhydrous (Na_2HPO_4, ≥ 99.9%) from Merk KGaA (Darmstadt, Germany), sodium dihydrogen phosphate anhydrous (NaH_2PO_4, ≥ 99.9%) from Fluka™ Analytical (Noth Carolina, US), triphenylene pro analysis (≥ 98%) from Sigma Aldrich (Missouri, US), sodiumfluoride (NaF, ACS reagent, ≥ 99%) from Merck KGaA (Darmstadt, Germany), LiChrosolv® *N,N*-dimethylformamide (DMF, for liquid chromatography) Merck KGaA (Darmstadt, Germany).

The blank rat plasma (with K_2EDTA as anticoagulant) was provided by Irena Loryan, M.D., PhD (Uppsala University, Department of Pharmaceutical Biosciences, Translational PKPD Group, Sweden). The blank human plasma (with citrate as anticoagulant) was purchased from VWR International (Pennsylvania, US). All plasma was delivered to Vienna University and stored at -80 °C in Eppendorf tubes until usage.

2.2. Equipment and materials

The analytes for the stock solutions were weighed on a MC210 analytic balance by Sartorius Lab Instruments GmbH & Co. KG (Goettingen, Germany). For plasma sample preparation a 5804 R centrifuge by Eppendorf (Hamburg, Germany) and an Extraction Plate Manifold for Oasis® PRIME HLB *µ*Elution Plate with 96 wells from Waters™ (Massachusetts, US) for SPE was used. In terms of plasma sample incubation, a Thermomixer® comfort by Eppendorf (Hamburg, Germany) was set to 37 °C and mix. Additionally, a pHenomenal® pH/mV/ °C/ion Meter IS2100L with a pHenomenal® 221 662-1161 electrode from VWR International (Pennsylvania, US) was used.

An Nexera XRultra high performance liquid chromatography (UHPLC) system by Shimadzu (Japan) was used for gradient optimization. It consists of DGU-20A5R degassing unit, two LC-20AD XR liquid chromatography pumps, SIL-20A XR autosampler, CTO-20AC prominence column oven, SPD-M20A prominence diode array detector (set to 254 nm) and CBM-20A prominence communications bus module. For the whole of this study a RP-HPLC setting was used. Mobile phase was generated according to the gradient with acetonitrile (LC-MS grade) and acidic water (0.1% formic acid, LC-MS grade). A 50 x 2.1 mm Kinetex® 2.6 *µ*m Phenyl-Hexyl 100 LC column with an AJ0-8788 Ph 6 filter by Phenomenex® Inc. (California, US) was used for separation. The data was analysed using Lab Solutions from Shimadzu (Japan).

The used LC-HRMS set up for measuring various drug plasma concentrations consists of an Ultimate 3000 RSLC-series system by Thermo Fisher Scientific™ Dionex™ (Gemering, Germany) paired with an maXis electrospray ionization double quadrupole mass analyser time-of-flight mass spectrometer by Bruker Corporation (Bremen, Germany). All parts of the UHPLC system were from the Dionex™ UltiMate 3000 product line and is set up of SRD-3400 degassing unit, RS pump, RS autosampler, RS Column Compartment, RS Diode Array Detector (set to 254 nm).
Mobile and solid phase were the same as for the gradient optimisation, described above.

The data was analysed using Compass DataAnalysis 4.2 by Bruker Corporation (Bremen, Germany).

For the determination of logP another HPLC system by Shimadzu (Japan) was used. It consists of a LC-20AD XR pump, DGU-20A3R degassing unit, SIL-20AC HT autosampler, CTO-20AC column oven, SPD-M20A diode array detector (set to 254 nm) and CBM-20A communication bus module. A Shim-pack GIST 3 μm C18 column (4.6 x 50 mm) from Shimadzu (Japan) was used with a phosphate buffer (pH 7.4) and methanol as mobile phase.

2.3. UHPLC - Method setting and conditions

The RP-UHPLC conditions used for gradient optimisation can be seen in Table 1. The conditions were set to 0.400 mL/min flow (resulting in approximately 170 bar pump pressure), 40 °C oven temperature and 10 μL injection volume.

Table 1. RP-UHPLC conditions used for the gradient optimisation. The solvents (Solvent A – acidic water (0.1% formic acid, LC-MS grade), Solvent B – acetonitrile (LC-MS grade)) were mixed according to the gradient settings.

Item	Value	Units
Mode	Binary gradient	
Total flow	0.400	mL/min
Pump A Pressure	172	bar
Pump B Pressure	171	Bar
Pump A Degassing	-95	kPa
Pump B Degassing	Not connected	
Oven Temperature	40.0	°C
Temperature L	60	°C
Injection Volume	10	μL
Overlap Mode	off	

2.4. Method and settings for LC-HRMS measurements

For the LC-MS measurements the parameters were also set to 0.400 mL/min flow, 170 bar pump pressure, 40 °C oven temperature and 10 μL injection volume. Measurements were performed along a previous applied gradient (Table) with acidic water (0.1% formic acid, LC-MS grade) and ACN (LC-MS grade).

The raw data gained from the LC-MS was analysed with the DataAnalysis 4.2 software by Brucker Cooperation. For each sample extracted ion chromatograms (EIC) at 167.084±0.01 *m/z* (*R*-MO), 297.054±0.01 *m/z* (MA), 314.064±0.01 *m/z* (*S*-CE-123) and 328.079±0.01 *m/z* (CE-137) were generated and further analysed. Slight changes in the last two decimal places (±0.03 *m/z*) of the *m/z* ratio for each substance are acceptable due to ionisation differences.

As the ionisation efficacy of the analytes can vary between different runs, the structurally similar compound CE-137 was selected as internal standard (IS). Each sample and calibration standard was spiked to a final concentration of 500 ng/mL of CE-137 and integrated analyte area was divided by the integrated CE-137 area of to ensure comparability over the course of this study.

The signal-to-noise ratio (S/N ratio) was calculated by the analysing software by comparing the signal intensity to the background noise of the EIC. Two lower limits were set according to the ICH guidelines, the limit of detection (LOD) = 3 and the limit of quantification (LOQ) = 10 to ensure measurement integrity [39].

Each batch started by injecting and measuring three blanks, two quality control (QC) samples and another blank before the actual samples. The batch ended with another blank, two QC samples and another blank. The blank consists of 500 µL ACN 70% and 500 µL acidic water (0.1% formic acid) as used in the final step of SPE sample preparation. The QC sample consists of 498 µL of each ACN 70% and acidic water (0.1% formic acid) spiked with 1 µL of each *R*-MO, MA, *S*-CE-123 and CE-137 stock solutions [c(analyte) = 1 µL/mL]. By comparing the area(analyte)/area(IS) of the before- and after-samples QCs, the measurement consistency throughout the batch could be guaranteed. The before and after QCs were not allowed to differ more than ± 15%.

2.4.1. Fragment ions of the analytes

Table 2 shows the *m/z* ratios of formed fragment ions of *R*-MO, MA, *S*-CE-123 and CE-137 as well as the molecular mass of the parent ion. As these compounds are structurally very similar, they all dissociate to a 167.084 *m/z* fragment, which is most probably the diphenylenmethyl rest. To avoid peak overlapping in the respective extracted ion chromatogram all substances should be separated by UHPLC before entering the MS. While, no stable $[M+H]^+$ form of the whole *R*-MO molecule could be detected, the fragment ion was used for quantification. For MA the Na^+ adduct was used for quantification.

Table 2. List of molecular mass of the parent ion and typical *m/z* ratios of formed ions for each analyte. *R*-MO - *R*-modafinil, MA - modafinil acid.

Analyte	Molecular mass [g/mol]	*m/z* ratio of formed ions
***R*-MO**	273.35	167.084 $[M+H]^+$ 296.069 $[M+Na]^+$
MA	274.36	167.084 $[M+H]^+$ 297.054 $[M+Na]^+$
***S*-CE-123**	313.47	167.084 $[M+H]^+$ 314.064 $[M+H]^+$
CE-137	327.50	167.084 $[M+H]^+$ 328.079 $[M+H]^+$

2.5. Stock solution preparation

The used stock solutions of *R*-MO, MA, *S*-CE-123 and CE-137 were all prepared by weighing 10.06 mg, 10.07 mg, 10.04 mg and 9.98 mg, respectively and dissolving each in a 10 mL Erlenmeyer flask with acetonitrile. The flasks were subsequently put in an ultrasound bath for five minutes to ensure complete solvation. The weigh-ins led to concentrations of 1.006 mg/mL, 1.007 mg/mL, 1.004 mg/mL and 0.998 mg/mL, respectively. The exact concentrations were considered when calculating sample concentrations.
Any other stock solutions used in this study were prepared accordingly and stored at -20 °C for maximum three months until usage.

2.6. Calibration standard preparation

For the quantification of *R*-MO, MA and *S*-CE-123 calibration curves with at least six different initial concentrations were prepared and measured. In alignment with the results of the screening experiment in rat plasma (section 3.2) the range for *R*-MO was set between 100-4000 ng/mL, for MA between 200-2000 ng/mL and for *S*-CE-123 between 100-1500 ng/mL. The described protocol was used for establishing calibration curves in rat and human plasma.

2.6.1. Master mixes

Intermediate solution A of internal standard (CISA, 50 µg/mL) was prepared in an Eppendorf tube by spiking 95 µL ACN 100% with 5 µL *S*-CE-137 stock solution (1 mg/mL). Further 990 µL ACN 100% were spiked with 10 µL of CISA to gain ACN-internal standard solution (AST, 500 ng/mL). Due to buffer – ACN incompatibility, MeOH was used instead of ACN for the protein precipitation of human plasma samples – MeOH-internal standard solution (MeST, 500 ng/mL).

The ice-cold plasma was used for preparation of master mix solutions. The preparation followed Table 3. The intermediate solution (e.g. ISB, ISC, ISD) was received by spiking blank plasma with the desired analyte stock solution in an Eppendorf tube. After vortexing, a certain volume of intermediate solution was used to spike blank plasma to get the main master mix (CM3, CMA, CMC). This step was repeated with the main master mix to get one diluted master mix (M3I, MAI, MCI) of each analyte. All intermediate solutions and master mixes were stored on ice until usage.

2.6.2. Spiking

The calibration standards were prepared in duplicate and were spiked with the prepared master mixes (section 2.6.1) following Table 4.
Blank plasma was put into the labelled Eppendorf tubes if needed and then spiked with respective master mixes to establish standards containing the desired concentration of *R*-MO, MA and *S*-CE-123.

Table 3. Preparation of intermediate solutions (ISB, ISC, ISD) and calibration master mixes (CM3, M3I, CMA, MAI, CMC, MC1 - marked grey), which were later used for establishing calibration standards. V – volume, c - analyte concentration in master mix

Analyte	Master mix name	Spiking	V (blank plasma) [µL]	c (analyte) [ng/mL]
***R*-MO**	ISB	5 µL of R-MO stock solution (1 mg/mL)	45	100 000
	CM3	15 µL of ISB	135	10 000
	M3I	10 µL CM3	90	1000
MA	ISC	5 µL of MA stock solution (1 mg/mL)	95	50 000
	CMA	25 µL of ISC	225	5000
	MAI	10 µL CMA	10	2500
***S*-CE-123**	ISD	5 µL of S-CE-123 stock solution (1 mg/mL)	95	50 000
	CMC	15 µL of ISD	135	5000
	MCI	5 µL CMC	45	500

Table 4. The table states the initial concentration (iC), and the needed volume of R-MO, MA, CE-123 respectively, V – volume, mast. mix – master mix

STD No.	***R*-MO**			**MA**			***S*-CE-123**				
	iC [ng/mL]	Mast. mix	V (mast. mix) [µL]	iC [ng/mL]	Mast. mix	V (mast. mix) [µL]	iC [ng/mL]	Mast. mix	V (mast. mix) [µL]	V (plas) [µL]	total V [µL]
0	0			0			0			50	50
1	100	**M3I**	5	200	**MAI**	4	100	**MCI**	10	31	50
2	200	**M3I**	10	500	**CMA**	5	500	**CMC**	5	30	50
3	500	**M3I**	25	800	**CMA**	8	800	**CMC**	8	9	50
4	1000	**CM3**	5	1200	**CMA**	12	900	**CMC**	9	24	50
5	2000	**CM3**	10	1600	**CMA**	16	1000	**CMC**	10	14	50
6	3000	**CM3**	15	2000	**CMA**	20	1500	**CMC**	15	0	50
7	4000	**CM3**	20	3000	**CMA**	30				0	50

After spiking and vortexing, 50 µL AST were added to each of the tubes and vortexed carefully. The samples were centrifuged for 10 minutes at 3000 x *g* and 4 °C. 25 µL of supernatant each were transferred into clean tubes and diluted with 225 µL H_2O + 0.1% FA. The dilution is necessary as high ACN concentrations in the supernatant result in the analytes being flushed through the cartridge with insufficient retention and therefore insufficient separation of parent compound and metabolite.

2.6.3. Solid phase extraction

The removal of the biological matrix (e.g. various proteins and lipids) was achieved by carrying out SPE purification.
The needed number of wells of a 96-well µElute plate were preconditioned with 200 µL ACN and equilibrated with 200 µL H_2O+0.1% FA. For each calibration standard, 250 µL, was loaded on an individual well. The wells were then washed twice with 200 µL H_2O+0.1% FA and once with 200 µL 10% ACN (in acidic water). The waste collection plate in vacuum manifold was switched to 700 µL 96-well plate. The analytes were eluted by two times 25 µL 70% ACN (in acidic water) and diluted with 50 µL H_2O+0.1% FA (total volume: 100 µL), followed by the measurement according to the LC-HRMS method.

2.7. Method validation

Method validation is an important tool to increase the consistency and quality of obtained results with a certain analytical method.

The detection limit (LOD) and quantification limit (LOQ) were based on the Signal-to-Noise (S/N) ratio of gained HRMS results. According to the ICH guidelines the S/N-ratio for LOD of the lowest concentration is to be at least 3 to be considered acceptable. This ensures that potential baseline noise is not mistakenly seen as analyte signal. To guarantee appropriate quantification the S/N-ratio for LOQ is to be at least 10 [40].

The method was validated according to the ICH guideline M10 for bioanalytical methods (2019) [39]. This was done with calibration standards in rat plasma. The calibration curve was to be set up of at least 6 concentrations and one blank sample. The sample preparation for all calibration standards (section 2.6) was carried out three times on different days and measured with HRMS, whereas sample preparation and measurements had to be done on the same day at least once.
The between-run precision and accuracy were determined by choosing 4 standards of the calibration. The average and standard deviation (SD) of all individual results from the same concentration level were calculated. The SD was divided by the average multiplied by 100 to gain the between-run precision [%]. The accuracy [%] was calculated by calculating the actual (true) concentration of each sample and dividing it by the target concentration and multiplied by 100. For all four concentration levels precision and accuracy were to be within ± 15% and ± 20% at lower limit of quantification – LLOQ.

2.8. Incubation sample preparation

For generating plasma curves, samples with the same initial concentration (iC) of the drug were incubated for various times. Two samples were prepared for each incubation time and measured in duplicate.

The following describes the preparation for all plasma stability experiments. The AST was prepared as described in section 2.6 and 18 Eppendorf tubes for the *R*-MO samples were prepared with 40 µL blank plasma and pre-warmed at 37 °C for 5 min to ensure immediate reaction start once the drug was added. 45 µL cold blank plasma were spiked with 5 µL of cold *R*-MO stock solution to receive Intermediate Solution A (ISB, 100 µg/mL). Further 180 µL cold blank plasma was spiked with 20 µL of ISB to gain the Master Mix Modafinil (M3, 10 000ng/mL). 10 µL of M3 were then added to each of the pre-warmed Eppendorf tubes and vortexed (iC = 2000 ng/mL). 50 µL ice-cold AST were added to 2 of the samples (t = 0.00 h, reaction start *R*-MO), carefully vortexed and frozen at -20 °C. The remaining samples were incubated in a Thermomixer® at 37 °C for 0.75, 1.50, 2.25, 3.00, 4.00, 5.00, 6.00 and 8.00 h. For each time, two of the incubated samples were taken out, the reaction stopped by adding 50 µL AST, carefully vortexed and stored at -20 °C until measurements.

For the *S*-CE-123 samples 10 Eppendorf tubes with 40 µL blank plasma were also pre-warmed at 37 °C for 5 min. Intermediate solution C (ISC, 50 µg/mL) was gained by spiking 95 µL cold blank plasma with 5 µL of *S*-CE-123 stock solution (1 mg/mL). 135 µL cold blank plasma were then spiked with 15 µL of ISC to receive Master Mix *S*-CE-123 (MC, 5 000 ng/mL). The pre-warmed Eppendorf tubes were each spiked with 10 µL of MC and vortexed (iC = 1000 ng/mL). The reaction in 2 of the samples was stopped immediately by adding 50 µL ice-cold AST, carefully vortexed and frozen at -20 °C (t = 0.00 h, reaction start *S*-CE-123). The remaining samples were also incubated at 37 °C for 2.00, 4.00, 6.00 and 8.00 h.

After finishing the incubation, samples were unfrozen and prepared for SPE purification like described in section 2.6.3.

2.9. Enzyme inhibition with DMF 10% and NaF 0.25%

For improving plasma stability of *R*-MO and *S*-CE-123 two enzyme inhibiting substances were compared. It was decided to trial with DMF 10% - as described by Gorman (2002) and Sesinova (2020) [33], [34] – and with NaF, described by Papoutsis *et al*. (2014) and Scheidweiler *et. al* (2000) [28], [31]. In terms of needed NaF concentration, these papers were contradictory. Papoutsis *et al*. (2014) added 100 mg NaF/5 mL blood sample before spiking with the substance of interest. Scheidweiler *et. al* (2000) tested 0.25 and 1% NaF and found 1% NaF no more effective than 0.25% NaF in stabilising their substance of interest, methylecgonidine. For this study it was decided to solve NaF in water before spiking blank rat plasma to ensure complete solvation. Due to the large NaF surplus in Papoutsis paper and the maximal solubility product of NaF in water (42 g/L) [41], it was decided to go with Scheidweiler's 0.25% NaF [31].

The DMF-plasma was prepared by spiking 1170 µL blank plasma with 130 µL DMF to gain a DMF plasma concentration of 10%. For the NaF-plasma a stock solution (c = 25.2 mg/mL) was prepared in water. After solvation 1170 µL blank plasma were spiked with 130 µL NaF stock solution to gain c = 2.52 mg/mL (i.e. 0.25%) NaF plasma concentration. All plasma was cooled on ice until usage.

2.10. Determination of lipophilicity *via* log P_{ow}

The determination of log P_{ow} was done following the log P_{ow} standard operating procedure (SOP) by Maisetschläger (2021) [42]. The adapted gradient is shown in Table 5. The method uses two standard substances with known log P_{ow} -values: log P_{ow} (toluene) = 2,69 and log P_{ow} (triphenylene) = 5,49 [43]. Due to their high lipophilicity the starting methanol concentration was increased to 60% to decrease their retention time (Rt). It was shortly discussed to change the organic mobile phase to ACN. Donovan and Pescatore (2002), however, stated that methanol gives higher correlation to log P_{ow} due to the ability to form hydrogen bonds [43]. Furthermore, a three-minute elution phase was added.

Table 5. Adapted gradient used for the determination of log P_{ow}. Conc – concentration, MeOH – methanol.

Time [min]	Conc. MeOH [%]	Conc. Phosphate buffer [%]
0.01	60	40
7.00	90	10
10.00	90	10
10.50	60	40
14.00	stop	

The phosphate buffer was prepared by dissolving 2.57 g Na_2HPO_4 and 1.46 g NaH_2PO_4 in 1 L water (HPLC grade). The pH was set to 7.4 with NaOH (4.4 M). 1.96 mg triphenylene were dissolved in 0.2 mL toluene and 20.0 mL MeOH to receive standard mix. For the samples 25 µL *R*-MO stock solution or *S*-CE-123 stock solution respectively were mixed in a 200 µL HPLC vial with 25 µL of standard mix, resulting in 500 µg/mL analyte concentration. Each sample was prepared and measured with the adapted gradient (Table 5) in triplicate under HPLC conditions shown in Table 6.

Table 6. HPLC conditions during the measurements for log P_{ow} of *R*-MO and *S*-CE-123.

Item	Value	Units
Oven temp	20	°C
Injection Volume	10	µL
Pump A Pressure	161	bar
Total Flow	1.2000	mL/min

The received Rt for *R*-MO and *S*-CE-123 respectively and for toluene and triphenylene were then used to calculate log P_{ow} using Equation 1.

Equation 1. Equation used to calculate logP of the analytes. log P_{ow} (toluene) =2.69 and log P_{ow} (triphenylene) = 5.49 are literature vales and like the equation were taken from Donovan and Prescatore (2002). Rt – retention time. [43]

$$logP_{analyte} = \frac{(logP_{toluene} - logP_{triphenylene}) * Rt_{analyte} + Rt_{toluene} * logP_{triphenylene} - Rt_{triphenylene} * logP_{toluene}}{Rt_{toluene} - Rt_{triphenylene}}$$

3. Results and Discussion

3.1. UHPLC gradient optimisation

Starting point was a UHPLC gradient developed by Tobias Strasser (2019) which in general showed good peak separation [44]. However, a better *R*-MO and MA peak separation would improve later analysis and precise quantification as both substances dissociate to the 167.084 *m/z* product ion. Due to their closeness in retention time this could lead to peak overlapping when analysing the extracted ion chromatograms after LC-MS measurements.

Table 7 shows Strasser's gradient with the exact mobile phase composition at certain time. The elution time between 1.50 and 5.50 min was set with an ACN concentration raise from 30 to 40%. The wash out phase started after the ACN increase to 95% at 6.00 until 12.00 min.

Table 7. UHPLC Gradient Strasser (2019) - ACN concentration during elution time increasing from 30 to 40%. Mobile phase A was acidic water (0.1% FA, LC-MS grade), mobile phase B was ACN (LC-MS grade) [44]. % V/V – volume percentage

Time [min]	Mobile phase A [% V/V]	Mobile phase B [% V/V]
0.01	95	5
1.00	95	5
1.50	70	30
5.50	60	40
6.00	5	95
8.00	5	95
8.20	30	70
9.20	30	70
10.00	95	5
12.00	--	--

As the focus lay on the separation of *R*-MO and MA only concentrations at the respective elution time (here between 1.50 and 5.50 min) were variated.

Experimental data showed that elongating elution time up to 10 minutes did not have significant effect on peak separation. However, after lowering the ACN concentration to 28-30 separation of the peaks improved. Due to the decrease of ACN, the retention time (Rt) of the substances was higher and the time settings had to be adjusted as well to ensure that none of them eluted during wash out phase. Table 8 shows the adapted ACN concentration and time settings.

The experiments showed that with the Kinetex® 2.6 μm Phenyl-Hexyl column further *R*-MO and modafinil acid peak separation is only possible by accepting broadened peaks and higher Rt. Decreasing the ACN concentration to 25-30% resulted in doubled peak width. Therefore, it is assumed that Gradient 1 reached maximal peak separation and acceptable peak appearance of these two substances with the used column.

Table 8. UHPLC Gradient 1 – ACN concentration during elution time increasing from 28 to 30%. Solvent A was acidic water (0.1% FA, LC-MS grade), solvent B was ACN (LC-MS grade). % V/V – volume percentage

Time [min]	Mobile phase A [% V/V]	Mobile phase B [% V/V]
0.01	95	5
1.00	95	5
1.50	72	28
4.00	70	30
6.50	65	35
7.50	5	95
9.50	5	95
9.70	30	70
10.70	30	70
11.50	95	5
13.50	--	--

A run with LC-MS at three different concentrations (100 ng/mL, 1000 ng/mL and 3000 ng/mL) showed that peak separation is indeed improved by Gradient 1 compared to Gradient Strasser (compare peak 1 and peak 2 of Chromatogram 1 and Chromatogram 2). However, when calculating theoretical parameters (shown in Table 9) like retention factor (k, Equation 2), selectivity (α, Equation 3), efficiency (N, Equation 4) and resolution (Rs, Equation 5) for both gradients, there is only little difference. A resolution of 1.5 is usually regarded as satisfactory for separating closely eluting substances [38] – which both gradients fulfil. The selectivity of Strasser's gradient has shown to be a slightly higher (0.9%), whereas the efficiency (12.5%) is lower and the resolution (0.9%) slightly lower.

Equation 2. Retention factor (k) is calculated for both peaks of interest (*R*-MO and MA) [38]. Rt – retention time of respective peak, t0 – retention time for unretained peak

$$k = \frac{(Rt - t0)}{t0}$$

Equation 3. Equation used to calculate selectivity (α) of the used method [38]. k_1 – retention factor *R*-MO, k_2 – retention factor of MA

$$\alpha = {k_2}/{k_1}$$

Equation 4. Efficiency (N) is calculated according to the German Pharmacopeia (A) or the United States Pharmacopeia (B) [38]. Rt – retention time (of *R*-MO), $w_{1/2}$ – peak width at half height, w – peak width at base

(A) $N = 5.54 * ({Rt}/{w_{1/2}})^2$ (B) $N = 16 * ({Rt}/{w})^2$

Equation 5. Equation to calculate the resolution (Rs) of each gradient [38]. N – efficiency, α – selectivity, k – retention factor (of *R*-MO)

$$Rs = \frac{\sqrt{N}}{4} * \frac{(\alpha - 1)}{\alpha} * \frac{k}{(k + 1)}$$

Table 9. Theoretical comparison of Gradient Strasser and Gradient 1. Calculated values of selectivity, efficiency and resolution each of the 3000 ng/ML sample. MO – *R*-modafinil, MA – modafinil acid

	Total time	**Rt (*R*-MO)**	**Rt (MA)**	**Selectivity (α)**	**Efficiency (N)**	**Resolution (Rs)**
Gradient Strasser	12.00 min	3.3 min	3.6 min	1.1304	6033.06	1.5616
Gradient 1	13.50 min	3.5 min	3.8 min	1.1200	6786.50	1.5762

As the Rs-values of both gradients do not significantly differ, the selectivity of Strasser's gradient is slightly better and its total running time is 1.50 min shorter it was decided to proceed with Strasser's gradient.

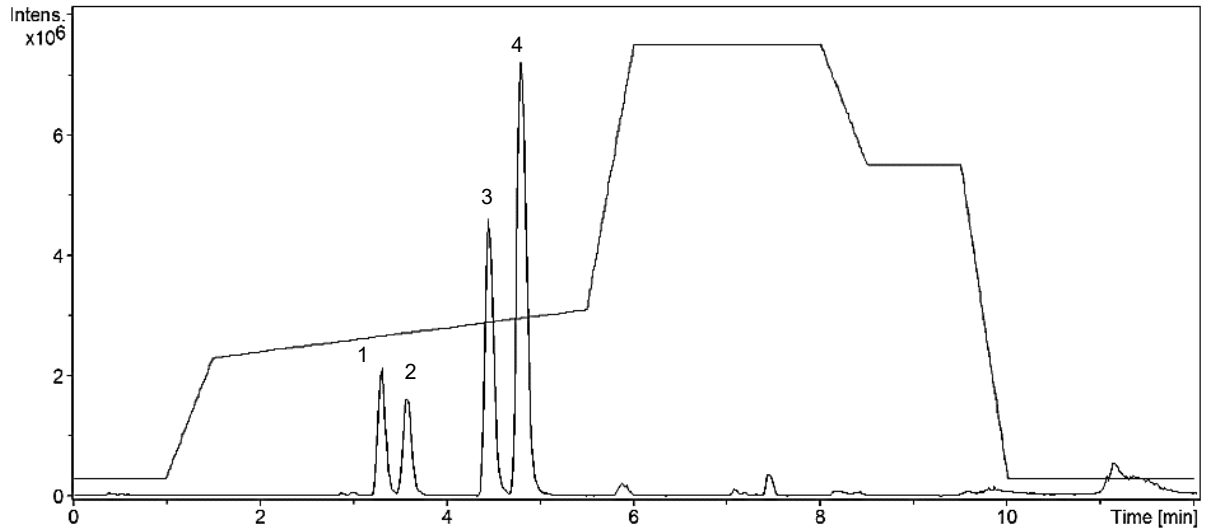

Chromatogram 2. LC-MS chromatogram of sample 3 (3000 ng/mL) measured with UHPLC Gradient Strasser (2019). The blue line shows the course of ACN concentration changes over the total running time (12.00 min). The black line shows the peaks of studied substances, whereas 1 – *R*-modafinil, 2 – modafinil acid, 3 – *S*-CE-123 and 4 – CE-137.

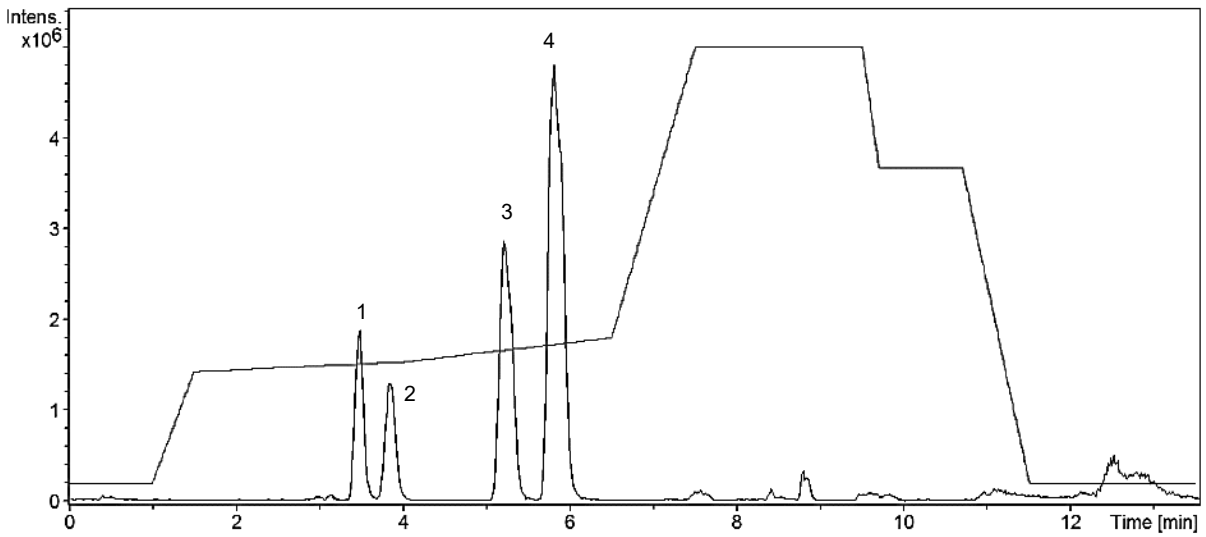

Chromatogram 1. LC-MS chromatogram of sample 3 (3000 ng/mL) measured with UHPLC Gradient 1. The blue line shows the course of ACN concentration changes over the total running time (13.50 min). The black line shows the peaks of studied substances, whereas 1 – *R*-modafinil, 2 – modafinil acid, 3 – *S*-CE-123 and 4 – CE-137.

3.2. Screening Experiments in rat plasma: Determination of time frame, analyte concentration and purification method

The aim of the first screening experiment was to determine the suitable time frame for examining plasma stability of *R*-MO and *S*-CE-123. As mentioned before the *in vivo* plasma half-life in humans of *R*-MO is approximately 15 hours.

The incubation time was decided to be set to 0, 9 and 18 h. The enzymatic reactions were stopped by adding ice cold AST (preparation see section 2.6) to achieve protein precipitation. As this was the first screening experiment 1000 ng/mL *R*-MO and *S*-CE-123 each were put together in samples to gain a general overview.

Figure 6 shows the area(analyte)/area(IS), which is proportional to analyte concentration, over the course of 18 hours experiment - the exact data is shown in Appendix Table 1. Coherently, the concentration of *R*-MO decreases for 92.5 % and of MA increases for 26.0 %, notably within the first 9 h of the experiment. The *S*-CE-123 concentration also decreases for 28.8 % - especially in the second half. This could potentially be explained by the availability of enzymes which were taken up by *R*-MO within the first 9 hours. To evaluate the actual *R*-MO and *S*-CE-123 metabolism, the two substances will consequently be incubated separately in following experiments. Following these results, the maximum incubation time was set to 8 hours.

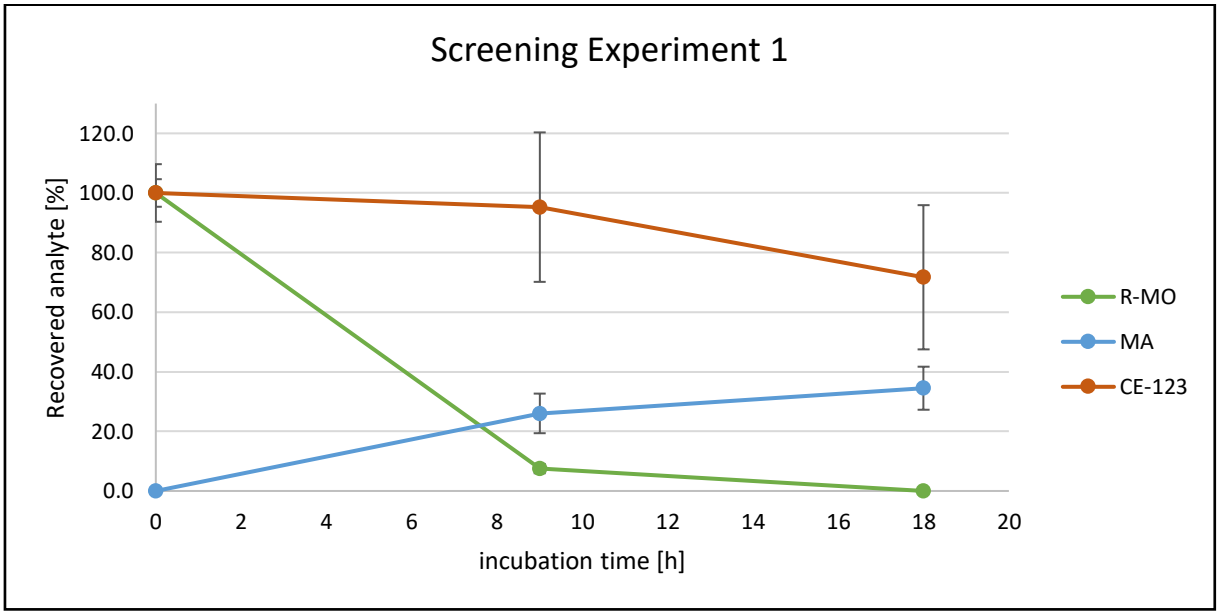

Figure 6. Results of Screening Experiment 1. 1000 ng/mL of *R*-MO and *S*-CE-123 each were incubated in rat plasma at 37 °C for up to 18 h. Area(analyte)/area(IS)-values plotted against incubation time 0, 9 and 18 h (n=3, average ± SD), error bars mark the standard deviation. Even though S/N-ratio of *R*-MO at 9 h was below LOQ, the data was still plotted for visualisation and screening purposes. The exact values are shown in Appendix Table 1. *R*-MO – *R*-modafinil, MA – modafinil acid, IS – internal standard

Even though the S/N-ratio of *R*-MO at 9 h was below LOQ, the data was still plotted for visualisation and screening purposes. The lower the concentration of drug in plasma the more difficult peak integration of *R*-MO and MA. Thus, the initial concentration of *R*-MO was set to 2000 ng/mL for the next experiment. Peak analysis of *S*-CE-123 signals was sufficient at 1000 ng/mL.

Screening Experiment 1 showed some difficulties in terms of peak analysis due to background noise. Therefore, the purification method SPE was conducted additionally to PP with half of the samples. To examine long term plasma stability of *S*-CE-123 an additional sample was added to the PP samples and incubated for 24 h.

Three samples of *R*-MO (2000 ng/mL) were incubated for 0, 4 and 8 h and four samples of *S*-CE-123 (1000 ng/mL) for 0, 4, 8 and 24 h.
Figure 7 shows the results of the PP-SPE-comparison. For this evaluation, the data after 4 hours incubation time was applied (exact data visible in

Appendix Table 2). There is a clear trend that detected values are higher with SPE. Furthermore, analyses/N ratios were found to be significantly higher in case of SPE sample preparation compared to PP and it is assumed that even lower analyte concentrations will be quantifiable. For these reasons, it was decided the additional purification step is worth the increased sample costs and time effort.

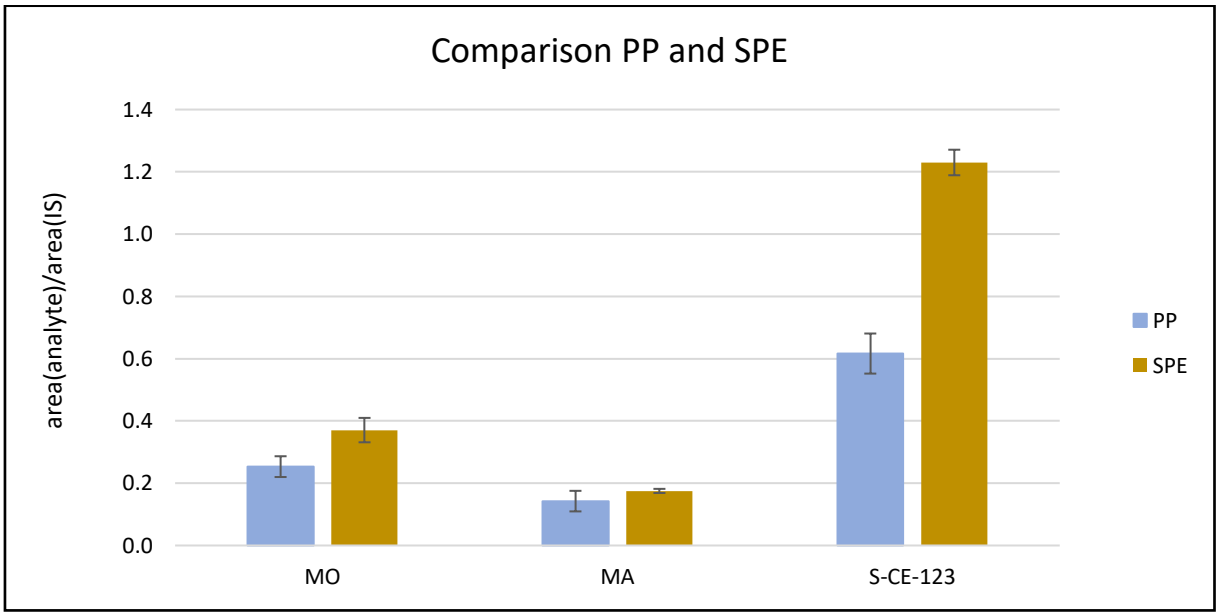

Figure 7. Comparison of protein precipitation (PP) and solid phase extraction (SPE). The detected data for PP and SPE after 4 hours incubation time is compared to each other (n=3, average ± SD), error bars mark the standard deviation. Exact data shown in Appendix Table 2. *R*-MO – *R*-modafinil, MA – modafinil acid, IS – internal standard

Additionally, *S*-CE-123 degradation was observed over 24 hours, whereas the samples were not purified with SPE. However, as shown in Figure 8, there was a discrepancy detected between the degradation results of *S*-CE-123 of PP and SPE after eight hours. The values of the PP samples were decreased by almost 48% within this time frame. In comparison, SPE samples even showed an increase of approximately 7% (exact data shown in Appendix Table 2). This trend was also detected in Screening Experiment 1 (data not shown).

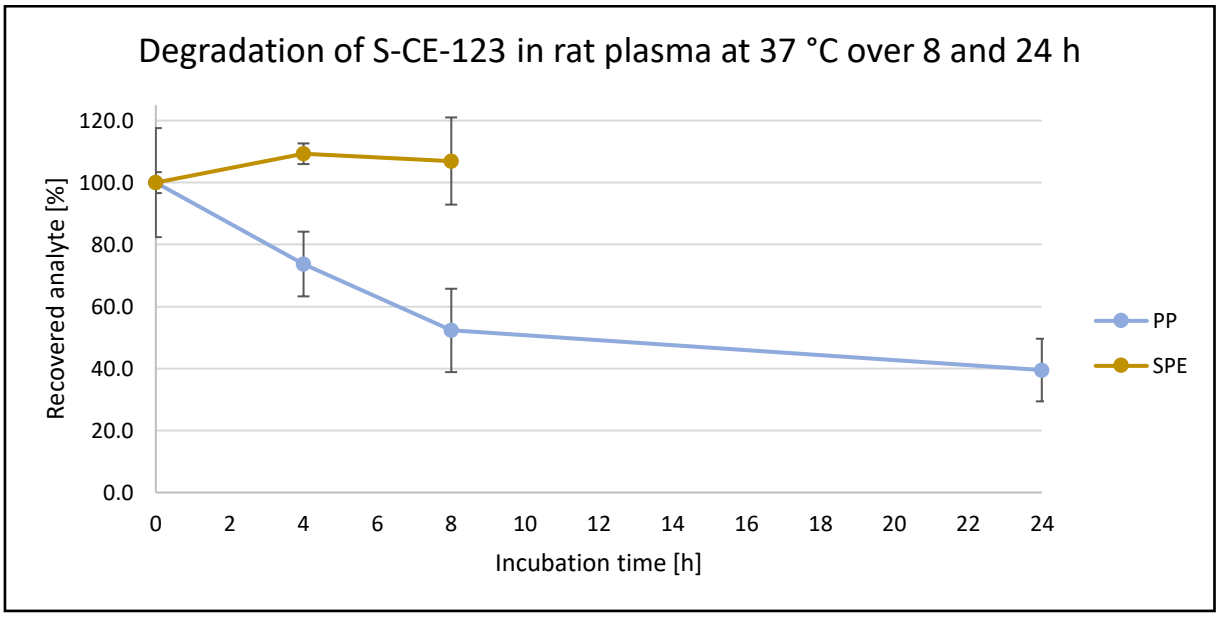

Figure 8. Degradation of incubated *S*-CE-123 in rat plasma at 37 °C. The detected percentages from protein precipitation (PP) and solid phase extraction (SPE) are plotted against incubation time (n=3, average ± SD), error bars mark the standard deviation. Exact data shown in Appendix Table 2. PP samples were incubated for 0, 4, 8 and 24 hours, SPE for 0, 4 and 8 hours.

It has to be mentioned that the used rat plasma contained K_2EDTA as anticoagulant instead of citrate in case of human plasma. EDTA interferes with substance ionisation during the LC-MS-measurements and leads to lower signals. This may explain the lower results of all PP samples in comparison with SPE and supports the decision mentioned above to purify all samples with SPE.

3.3. Calibration of *R*-MO, MA and *S*-CE-123 and their plasma stability in rat plasma

3.3.1. Calibration

Seven calibration standards for *R*-MO and MA and six standards for *S*-CE-123 were prepared in rat plasma in respective concentration ranges, like explained in section 2.6. The range for *R*-MO was set between 100-4000 ng/mL, for MA between 200-2000 ng/mL and for *S*-CE-123 between 100-1500 ng/mL. After preparation, the samples were purified with SPE, measured with LC-HRMS and validated according to the ICH guidelines M10 on bioanalytical method validation [39].

Figure 9 shows the calibration curve for *R*-MO between the concentration range 200-4000 ng/mL. Both the detected area and the concentration of analyte were divided by the detected area and concentration of the internal standard (IS, CE-137), respectively. The IS was added for compensating any losses during sample preparation and influences on ionisation increasing comparability of different samples and runs. Throughout the whole study the used concentration for IS was approximately 500 ng/mL.

The lowest measured concentration of *R*-MO (100.6 ng/mL) could be detected but not quantified and had to be excluded from the curve, as the accuracy (+ 110 %) was not within the acceptable range according to the ICH guideline (± 15% and ± 20% at lower limit of quantification - LLOQ). The accuracy of the 201.2 ng/mL *R*-MO standards was also out of range (Table 10). However, as the guideline states the calibration needs to be made up of six standards and 75% need to meet described requirements, the 201.2 ng/mL standard and the calibration are acceptable.

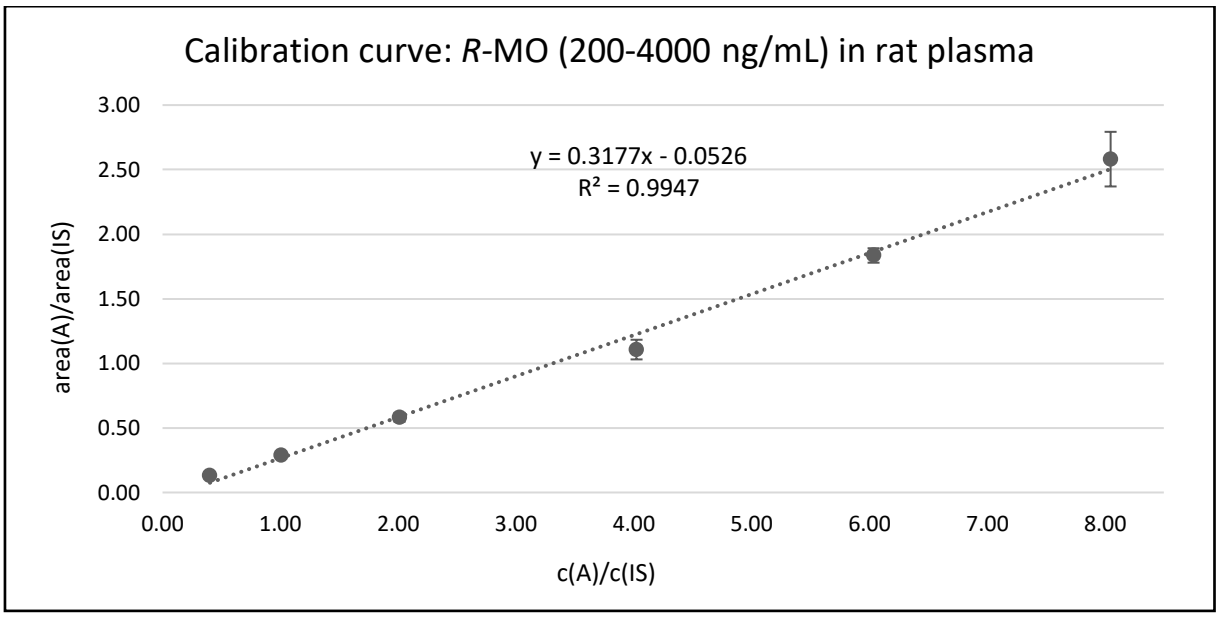

Figure 9. Calibration curve for *R*-MO in the range of 200-4000 ng/mL in blank rat plasma. The detected area and concentration of analyte were divided by the same of IS (n = 9, average ± SD). The individual values are shown in Appendix Table 3. A – analyte, IS – internal standard (CE-137)

Table 10. Precision and Accuracy of the calibration for *R*-MO (100-4000 ng/mL) in blank rat plasma. The grey marked value does not comply to ICH guidelines Individual values are shown in Appendix Table 3 (n = 9, average).

target conc. [ng/mL]	Precision [%]	Accuracy [%]
201.2	15	+ 43
503.0	12	+ 6
2012.0	5	- 9
3018.0	12	- 2

The calibration curve for MA between 200-3000 ng/mL is shown in Figure 10, the summary for its precision and accuracy in Table. Both the detected area and the concentration of analyte were again divided by the detected area and concentration of the internal standard (IS, CE-123), respectively.

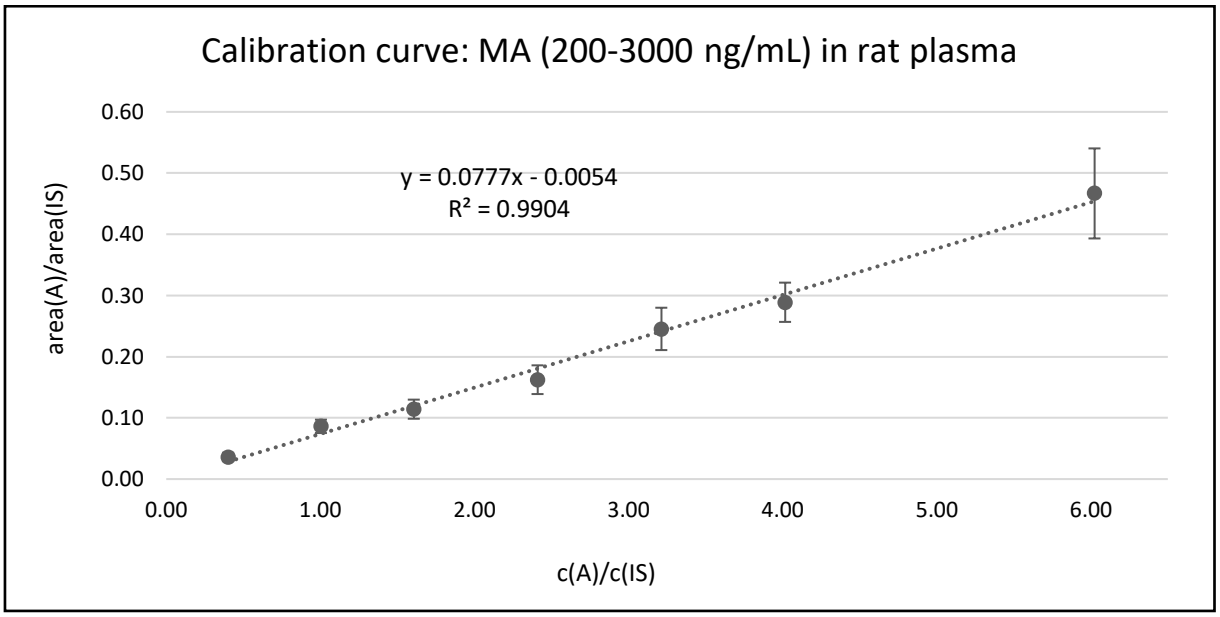

Figure 10. Calibration curve for MA in the range of 200-3000 ng/mL in blank rat plasma. The detected area and concentration of analyte were divided by the same of IS (n = 9, average ± SD). The individual values are shown in Appendix Table 4. MA – modafinil acid, A – analyte, IS – internal standard (CE-137)

The precision and accuracy of MA calibration is summarised in Table 11. All values except the accuracy of the 200.8 and 502.0 ng/mL standard (marked dark grey in Appendix Table 4) met the predetermined confident intervals for precision and accuracy as described before. The calibration is acceptable to the terms stated by the ICH guidelines.

Table 11. Precision and accuracy for the calibration of MA (200-3000 ng/mL) in blank rat plasma. The grey marked value does not comply to ICH guidelines. Individual values are shown in Appendix Table 4 (n = 9, STD 7 n = 8, average).

target conc. [ng/mL]	Precision [%]	Accuracy [%]
502.0	13	+ 17
803.2	14	- 4
1204.8	14	- 10
2008.0	11	- 6

Figure 11 shows the calibration curve for *S*-CE-123 in the range between 100-1500 ng/mL in rat plasma, Table 12the precision and accuracy analysis according to the ICH guidelines. All standards, except the accuracy of the lowest concentration (100.4 ng/mL, marked grey in Table 12) are within the suggested acceptance levels. As more than 75% of these standards meet the requirements the calibration is acceptable.

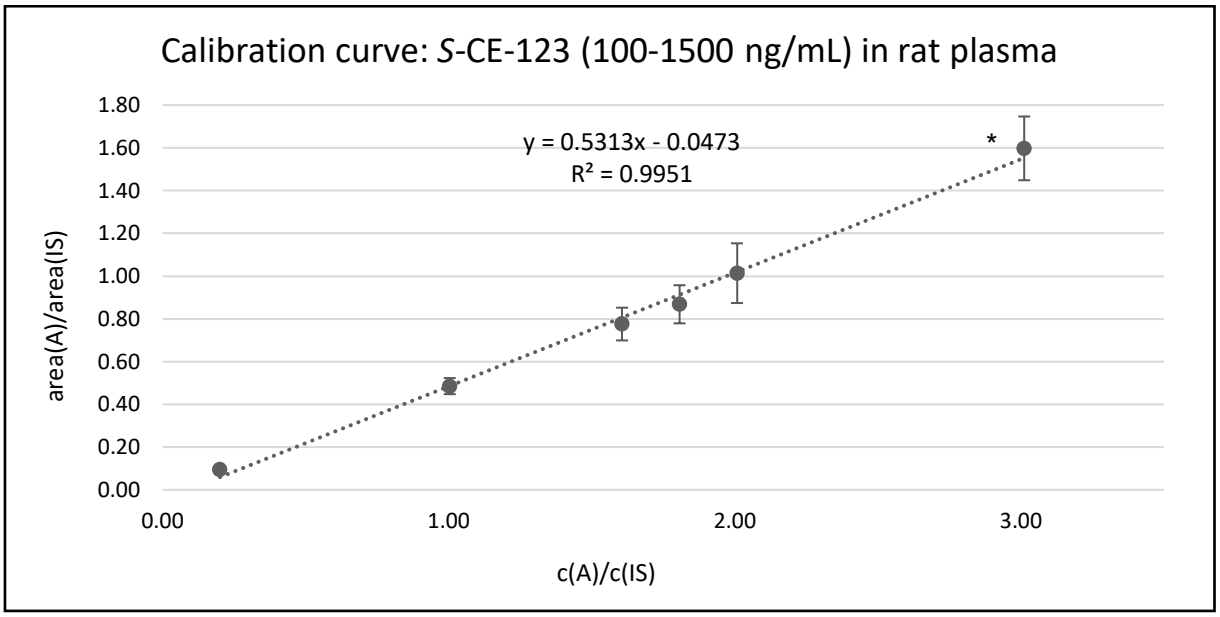

Figure 11. Calibration curve for *S*-CE-123 in the range of 100-1500 ng/mL in blank rat plasma. The detected area and concentration of analyte were divided by the same of IS (n = 9, * n = 8 for STD 6, average ± SD). The individual values are shown in Appendix Table 5. A – analyte, IS – internal standard (CE-137)

Table 12. Precision and accuracy of the calibration for *S*-CE-123 between 100-1500 ng/mL in blank rat plasma. The grey marked value does not comply to ICH guidelines Individual values are shown in Appendix Table 5 (n = 9, average).

target conc. [ng/mL]	Precision [%]	Accuracy [%]
100.4	15	+ 35
502.0	8	0
803.2	10	- 4
1004.0	14	- 1

3.3.2. Plasma stability of *R*-MO- and *S*-CE-123 in rat plasma

To determine the *in vitro* degradation rate of *R*-MO to MA in rat plasma, samples with the same initial concentration of 2000 ng/mL *R*-MO were incubated for different time periods. The incubation was stopped with AST after 0.75, 1.50, 2.25, 3.00, 4.00, 5.00, 6.00 and 8.00 h. As no significant degradation was expected when incubating *S*-CE-123 the incubation was stopped after 2.00, 4.00, 6.00 and 8.00 h, the initial concentration of the samples was 1000 ng/mL.

The integrated areas of analyte peaks were divided by the integrated area of IS peaks (CE-137). The average of the same incubation time was converted to c(A)/c(IS) using the linear equation for the corresponding analyte and then multiplied by the concentration of IS (500 ng/mL). The calculated *R*-MO and MA concentrations were referred to the recovered *R*-MO concentration at t = 0 h to receive the degradation and formation respectively based on *R*-MO in percent. The *S*-CE-123 concentrations were based on the recovered *S*-CE-123 concentration at t = 0 h. The exact values are shown in Appendix Table 6 for *R*-MO, Appendix Table 7 for MA and Appendix Table 8 for *S*-CE-123.

Figure 12 shows the plotted *R*-MO and MA percentages against the incubation time. The *R*-MO percentage (green) decreases rapidly and elimination half time ($t^1/_2$) is reached only after 1.5 h. The degradation rate significantly slows down after 4 h, most probably because of decreasing substrate (i.e. analyte) concentration. Due to the limits of the calibration, the *R*-MO concentration at 8 h could only be detected but not quantified. The percentage of MA (blue) gradually rises until the curve flattens after 6 h as there is less *R*-MO left to be transformed by plasma enzymes. In summary, 6.6±0.5% of *R*-MO was left after 8 h incubation and 78.3±2.2% of the initial *R*-MO concentration was metabolised to MA – assuming the ionisation for HR-MS measurements for *R*-MO and MA was complete.

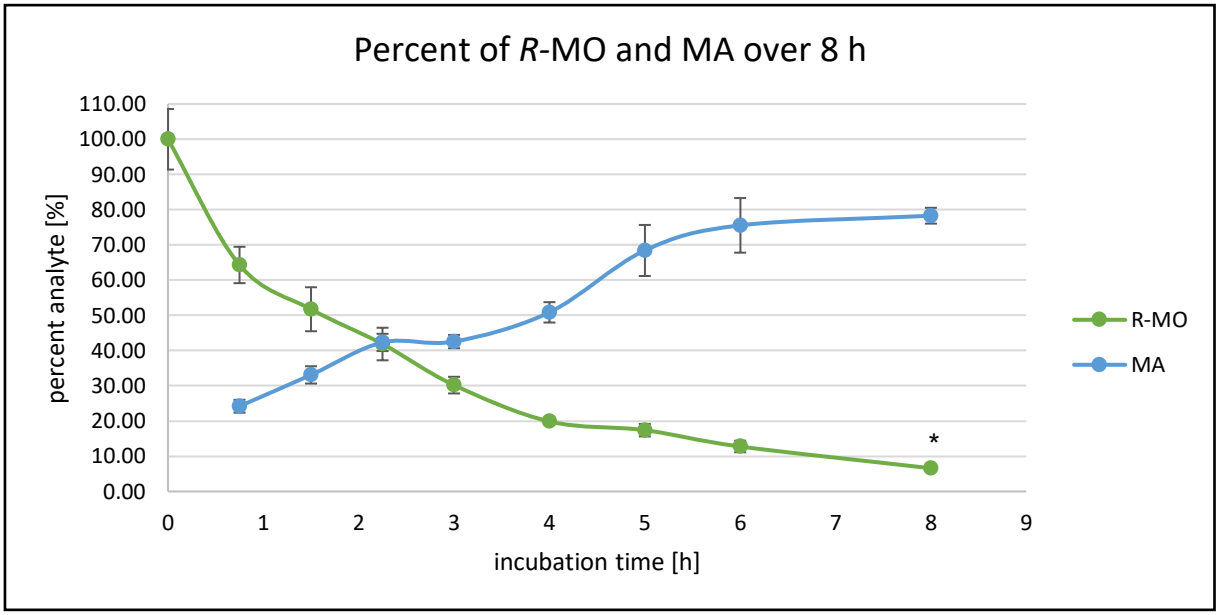

Figure 12. Results of incubation of *R*-MO in rat plasma at 37 °C over 8 h. The green data shows the degradation of *R*-MO and the blue the formation of MA. The percentage of formed MA was received by referring the recovered concentration of MA to the recovered *R*-MO concentration at t = 0 h (n = 3, average ± SD). * Concentration could be detected but not quantified. The individual values for *R*-MO are shown in Appendix Table 6 and for MA in Appendix Table 7. *R*-MO – *R*-modafinil, MA – modafinil acid

It was noticed that when adding the percentages of recovered *R*-MO and MA (all referred to the recovered *R*-MO concentration at t = 0 h), 100% recovery were never reached, as shown in Figure 13. The recovery varied between 70.73-89.28%. There are different potential reasons. Firstly, either not all MA was ionised and further not detected by MS. Secondly, the degradation of *R*-MO also causes the formation of metabolites other than MA which cannot be identified by used analytical methods. Lastly, MA itself gets metabolised by plasma enzymes. The last hypothesis is seconded by the results of Willavize *et al.* (2017), who studied the pharmacokinetics of armodafinil, MA and modafinil sulfone. It was found that the clearance of MA was more than 8 times and of modafinil sulfone more than 3 times that of the parent compound [45].

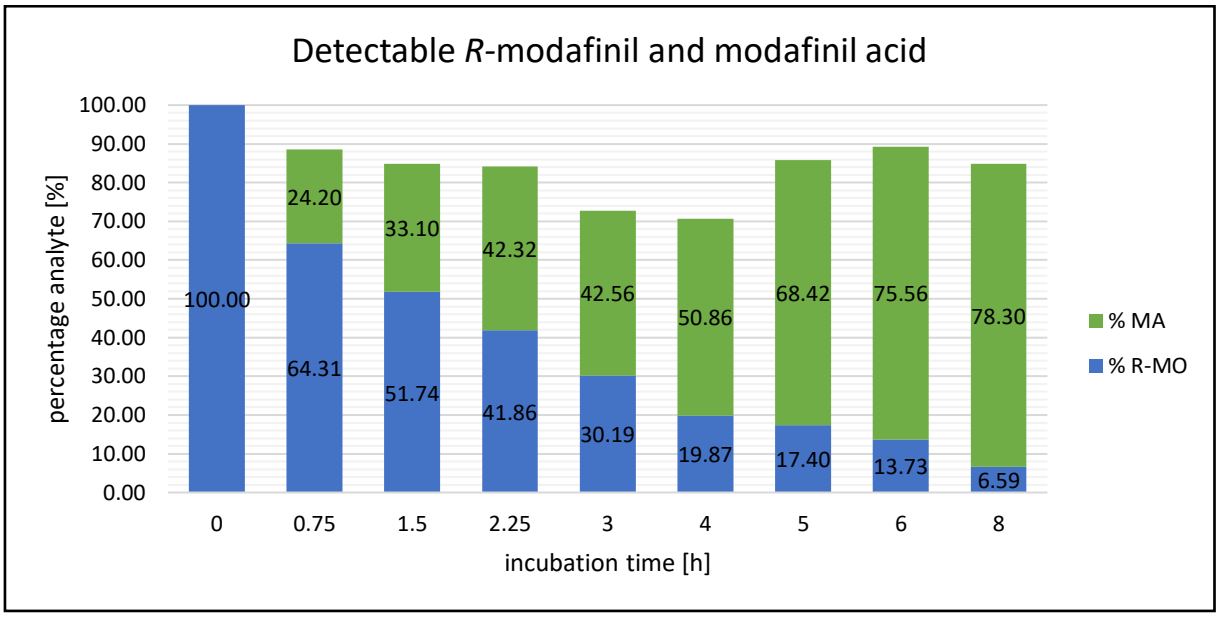

Figure 13. Percentages of detected *R*-MO and MA. All recovered concentrations of both data sets were referred to the recovered concentration of *R*-MO at t = 0 h (n = 3, average). The individual values are shown in Appendix Table 9. *R*-MO – *R*-modafinil, MA – modafinil acid

The results of the incubation of *S*-CE-123 in this experiment and the previous screening experiment showed no significant decrease in concentration, as shown in Figure 14. It can be concluded that this analogue of *R*-MO is not susceptible to the degradation by plasma enzymes within the given time period.

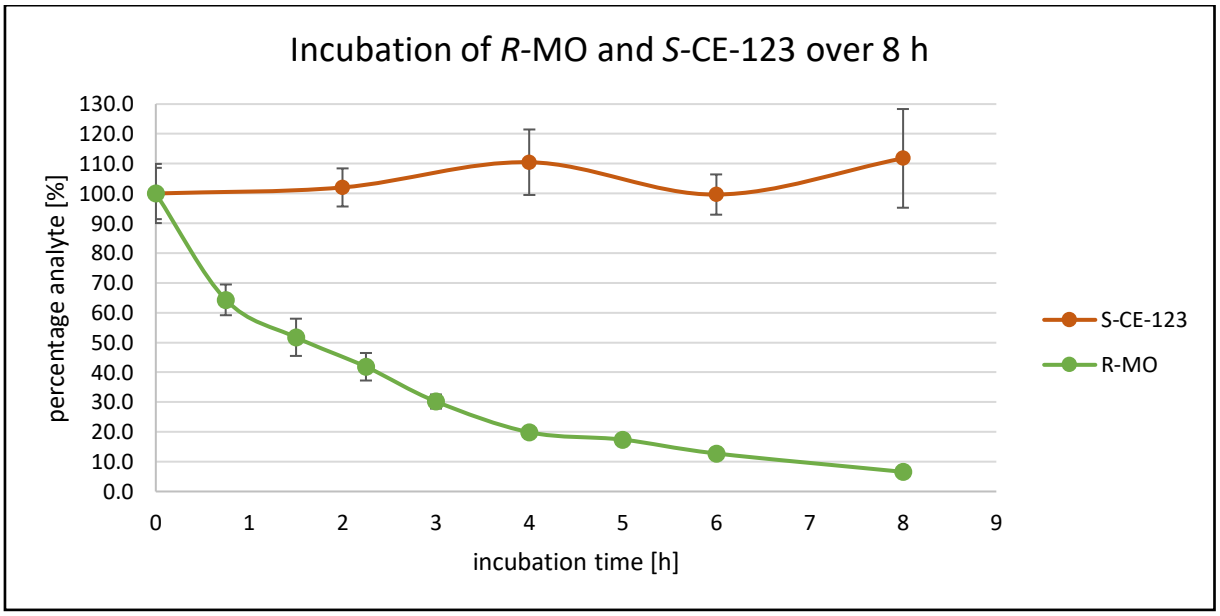

Figure 14. Results of incubation of *R*-MO and *S*-CE-123 in rat plasma at 37 °C over 8 h. The recovered concentrations of the incubated samples were referred to the respective recovered concentration at t = 0 h (n = 3, average ± SD) and then plotted against the incubation time. The individual values are shown in Appendix Table 6 for *R*-MO and Appendix Table 8 for *S*-CE-123. *R*-MO – *R*-modafinil

3.4. Enzyme inhibition with DMF 10% and NaF 0.25% in rat plasma

The blank rat plasma was spiked with DMF and NaF as described in section 2.9.
For the plasma stability in DMF-plasma, samples with initial concentration of 2000 ng/mL *R*-MO and 1000 ng/mL *S*-CE-123 were prepared and incubated for 0.00, 2.00, 4.00, 6.00 and 8.00 h. For NaF-plasma the same protocol was followed.
The results were processed as described in section 3.3.2.

Figure 15 compares the results of *R*-MO incubation in blank, DMF- and NaF-plasma. After 8 h incubation of *R*-MO at 37 °C 6.6±0.5% in blank plasma were left (green, data from earlier experiment - Figure 12). In DMF spiked plasma (blue) remained 66.8±7.2% of the initial *R*-MO after 6 h and 83.0±11.4% after 8 h. It was assumed that the result at 6 h is more accurate than the one at 8 h as it follows the trend set by the results at 2 and 4 h. The difference could be explained by the different efficacies of ionisation when analysing the samples. 38.0±22.8% of *R*-MO were left in the NaF spiked plasma (orange) after 8 h.

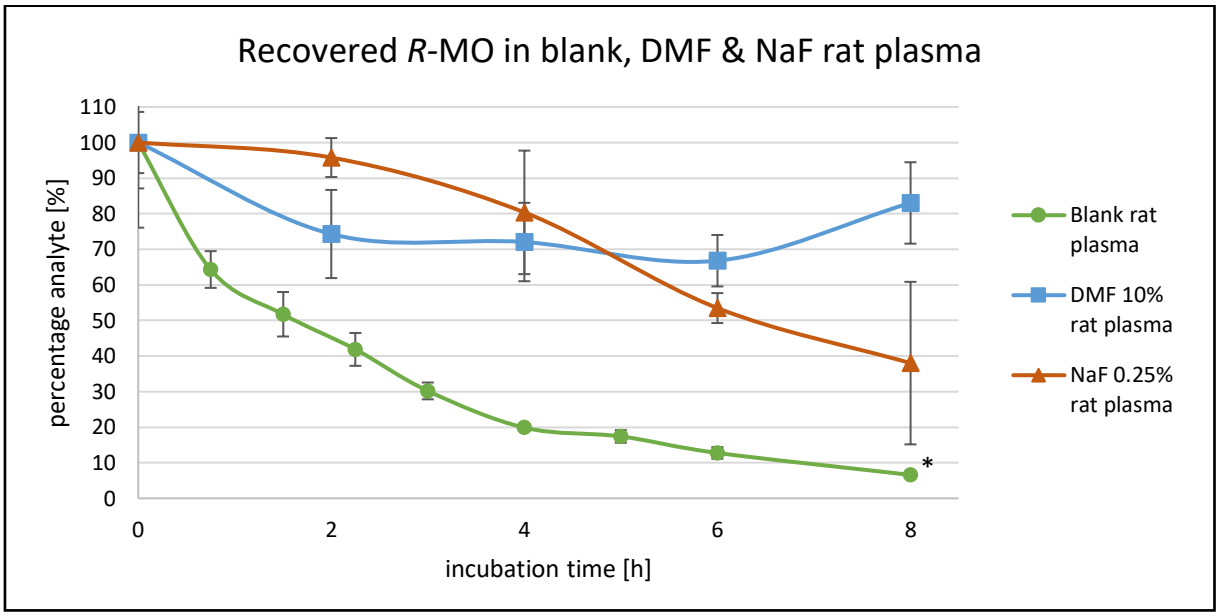

Figure 15. Results of incubation of *R*-MO in blank (green), DMF 10%- (blue) and NaF 0.25%-plasma (orange) at 37 °C over 8 h (n = 3, average ± SD). The recovered concentrations of the incubated samples were referred to the respective recovered concentration at t = 0 h and plotted against incubation time. * Concentration could be detected but not quantified. The individual values are shown in Appendix Table 6 for incubation in blank plasma, Appendix Table 10 in DMF-plasma and Appendix Table 13 in NaF-plasma. *R*-MO – *R*-modafinil, DMF – dimethylformamide, NaF - sodium fluoride

Comparing these results of *R*-MO loss in DMF plasma to Gorman (2002), the loss was found to be higher in the present study. Gorman (2002) reported the loss to be < 5,5% after 3 h at room temperature [33]. The higher loss can be explained by the difference in incubation temperature, as enzyme activity is higher at 37 °C than at room temperature (approximately 20 °C).

Coherently to the decreased *R*-MO degradation, the formation of MA in inhibited plasma was found to be significantly lower than in blank plasma (Figure 16). All recovered MA concentrations were referred to the recovered *R*-MO concentration at t = 0 h in the respective plasma type. After 8 hours, 78.3±2.2% MA were recovered in blank plasma (green) and almost 9.7±1.0% in NaF-plasma (orange). As only little MA was formed in DMF-plasma (blue) it could just be detected but not reliably quantified due to the low concentrations.

In conclusion, 10% DMF in rat plasma successfully inhibits enzymes responsible for MA formation and was found to be superior to 0,25% NaF.

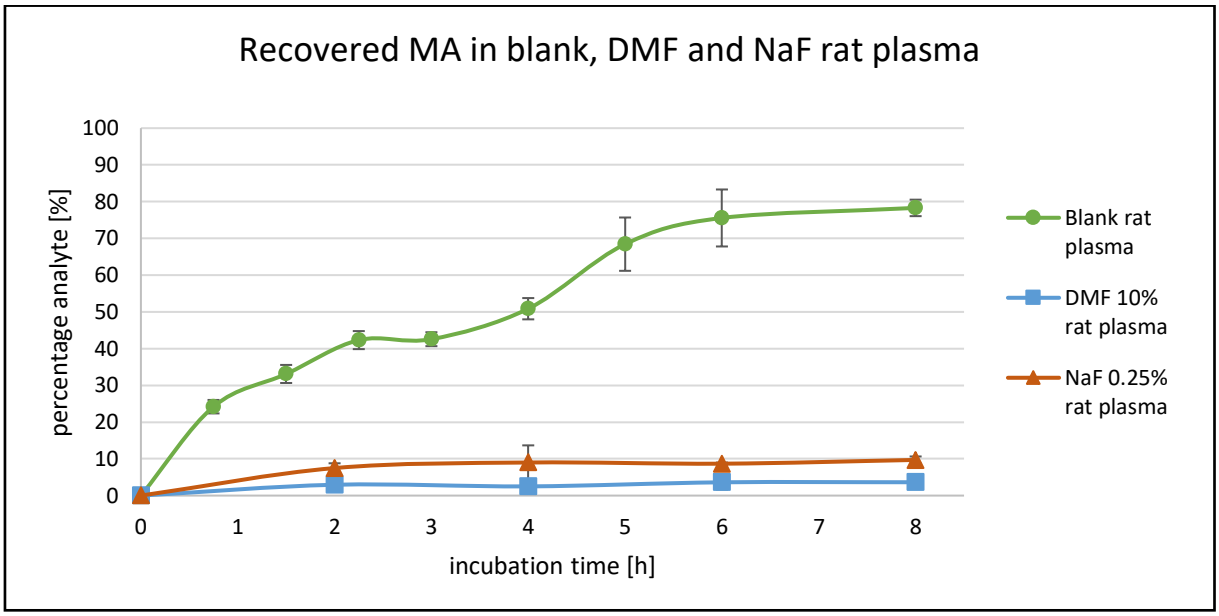

Figure 16. Formation of MA in blank (green), DMF 10%- (blue) and NaF 0.25%-rat plasma (orange) after incubating R-MO at 37 °C over 8 h (n = 4, average ± SD). The recovered concentrations of the incubated samples were referred to the respective recovered R-MO concentration at t = 0 h and then plotted against incubation time. The formed MA in DMF-plasma could not be quantified reliably and is only shown for visualising purposes. The individual values are shown in Appendix Table 7 for incubation in blank plasma, Appendix Table 11 in DMF-plasma and Appendix Table 14 in NaF-plasma. MA – modafinil acid, DMF – dimethylformamide, NaF - sodium fluoride

Figure 17 shows the incubation of *S*-CE-123 in blank, DMF 10%- and NaF 0.25%-spiked rat plasma. In line with all previous experiments, there was no significant effect of the inhibiting substances on the plasma stability of *S*-CE-123 observed.

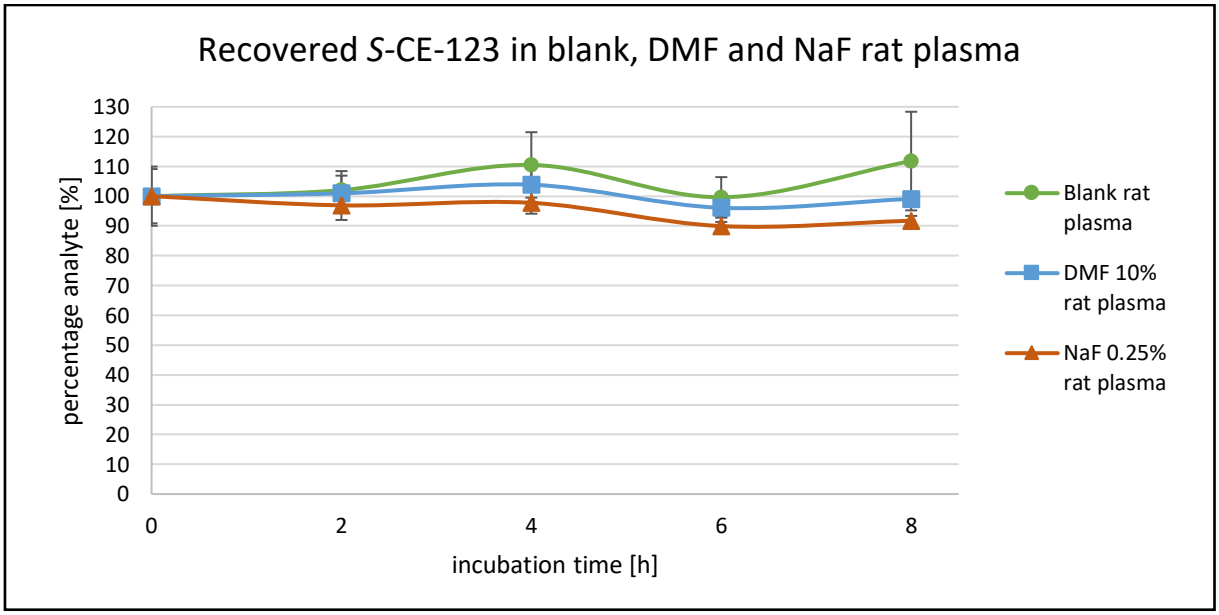

Figure 17. Results of incubation of *S*-CE-123 in blank (green), DMF 10%- (blue) and NaF 0.25%-rat plasma (orange) 37 °C over 8 h (n = 4, average ± SD). The recovered concentrations of the incubated samples were referred to the respective recovered concentration at t = 0 h and then plotted against incubation time. The individual values are shown in Appendix Table 8 for incubation in blank plasma, Appendix Table 12 in DMF-plasma and Appendix Table 15 in NaF-plasma. DMF – dimethylformamide, NaF - sodium fluoride

Even though both chosen substances were able to inhibit plasma enzymes, DMF 10% showed significantly higher inhibition efficiency compared to NaF 0.25% when incubating *R*-MO. Reasons could be either the higher concentration used in case of DMF or higher potency or affinity to the enzyme.

3.5. Human plasma stability of *R*-MO, MA and *S*-CE-123

As described in section 1.3, the plasma stability can differ between species. The aim of this study was to compare the plasma stability of *R*-MO and *S*-CE-123 in rat and human plasma. The validated calibration in rat plasma was also to be compared to the calibration in human plasma.

The purchased human plasma contained citrate as anticoagulant instead of K_2EDTA in rat plasma. The study done by Papoutsis *et al.* (2014) found no evidence that different anticoagulants effect the plasma enzyme activity [28]. However, previous experiments have shown that the combination of buffer and ACN lead to phase separation (results not shown). Since the analytes have different solubility in the organic and water phase, results would differ depending on which phase was used for SPE and could not be expected to be accurate. This issue could be resolved by substituting ACN for MeOH at the protein precipitation step.

3.5.1. Calibration

The calibration in human plasma was prepared and analysed like the one with rat plasma (section 2.6) with one exemption – MeOH instead of ACN for the protein precipitation. The range for *R*-MO was set between 100-4000 ng/mL, for MA between 200-2000 ng/mL and for *S*-CE-123 between 100-1500 ng/mL.

Figure 18 compares the calibration curves of *R*-MO in rat (200-4000 ng/mL, blue) and human plasma (100-4000 ng/mL, yellow). The human plasma calibration curve was not validated and precision and accuracy within the *R*-MO calibration curve did in general not meet the requirements stated by ICH guidelines (Appendix Table 16). However, both precision and accuracy in the concentration range of interest (around 2000 ng/mL for *R*-MO and 1000 ng/mL for *S*-CE-123, explained in the following section) comply.

In comparison of the linear equations, the slope in human plasma is nearly double the one in rat plasma, the intercept nearly four times higher than in rat plasma. Therefore, the *R*-MO calibration in rat plasma is not suitable for the quantification of human plasma samples.

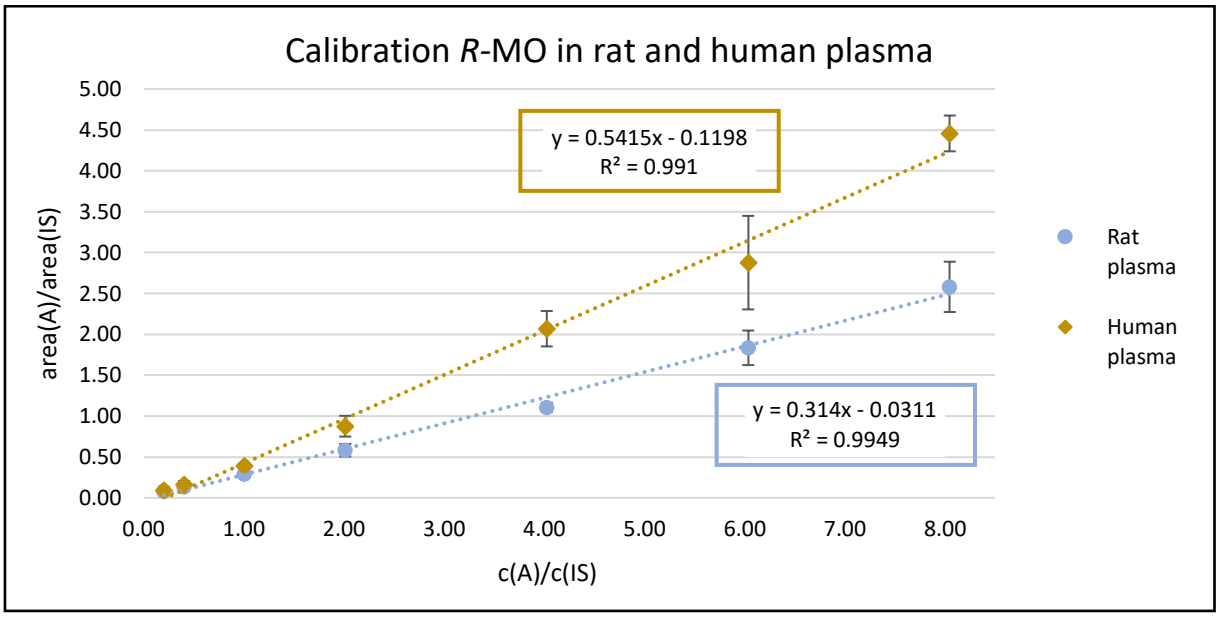

Figure 18. Calibration curve for *R*-MO in the range of 200-4000 ng/mL in blank rat (blue, n=9, average ± SD) and 100-4000 ng/mL human plasma (yellow, n=3, average ± SD). The detected area and concentration of analyte were divided by the same of IS. The individual values for rat plasma are shown in Appendix Table 3, for human plasma in Appendix Table 16. *R*-MO – *R*-modafinil, A – analyte, IS – internal standard (CE-137)

Figure 19 shows the calibration of MA in rat (200-3000 ng/mL) and human plasma (500-3000 ng/mL). The lowest MA standard (200 ng/mL) could not be detected in human plasma. While the accuracy within the unvalidated human plasma calibration curve complied to ICH guidelines, half of the standards did not comply to precision requirements (Appendix Table 17). When comparing linear equations, the slope of human plasma calibration is approximately 1/3 smaller, the intercept around 20 times higher than for the rat plasma calibration. Thus, the MA rat plasma calibration is not suitable for quantification of human plasma samples.

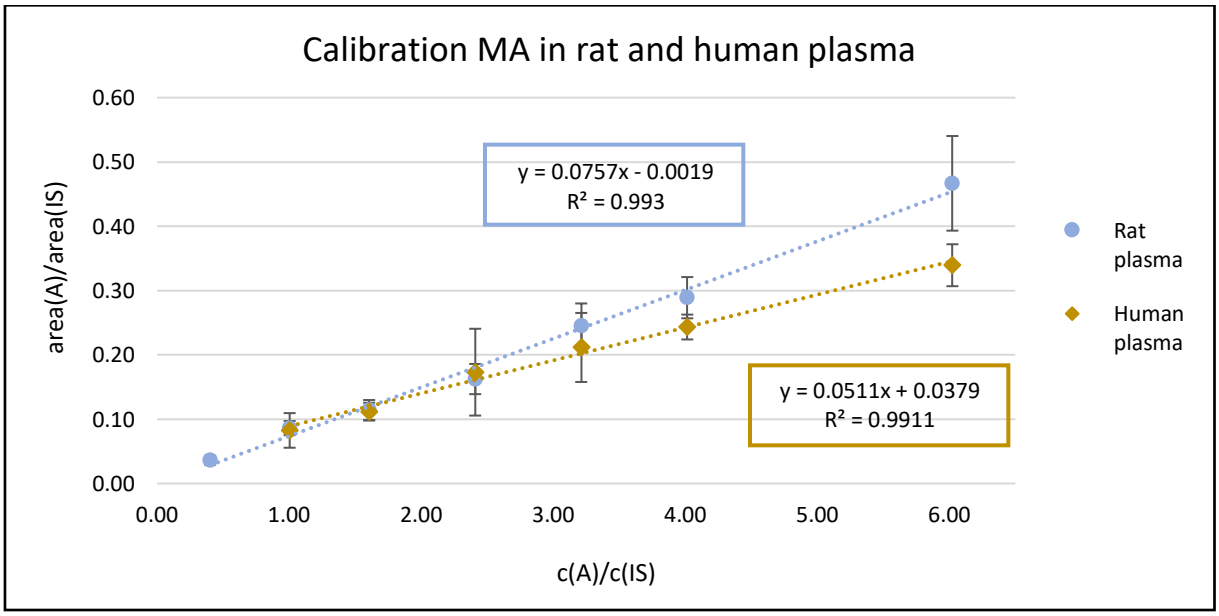

Figure 19. Calibration curve for MA in blank rat (200-3000 ng/mL, blue, n = 9, average ± SD) and human plasma (500-3000 ng/mL, yellow, n=3, average ± SD). The lowest concentration (200 ng/mL) could not be detected in human plasma. Detected area and concentration of analyte were divided by the same of IS. The individual values for rat plasma are shown in Appendix Table 4, for human plasma in Appendix Table 17. MA – modafinil acid, A – analyte, IS – internal standard (CE-137)

Figure 20 compares the calibration curves of *S*-CE-123 in rat and human plasma (100-1500 ng/mL). The accuracy within the human plasma calibration curve met requirements, the three lowest standards' precision did not comply (Appendix Table 18). There is no significant difference between the calibrations done in the two species. Therefore, the calibration in rat plasma can be used for the quantification of human plasma samples.

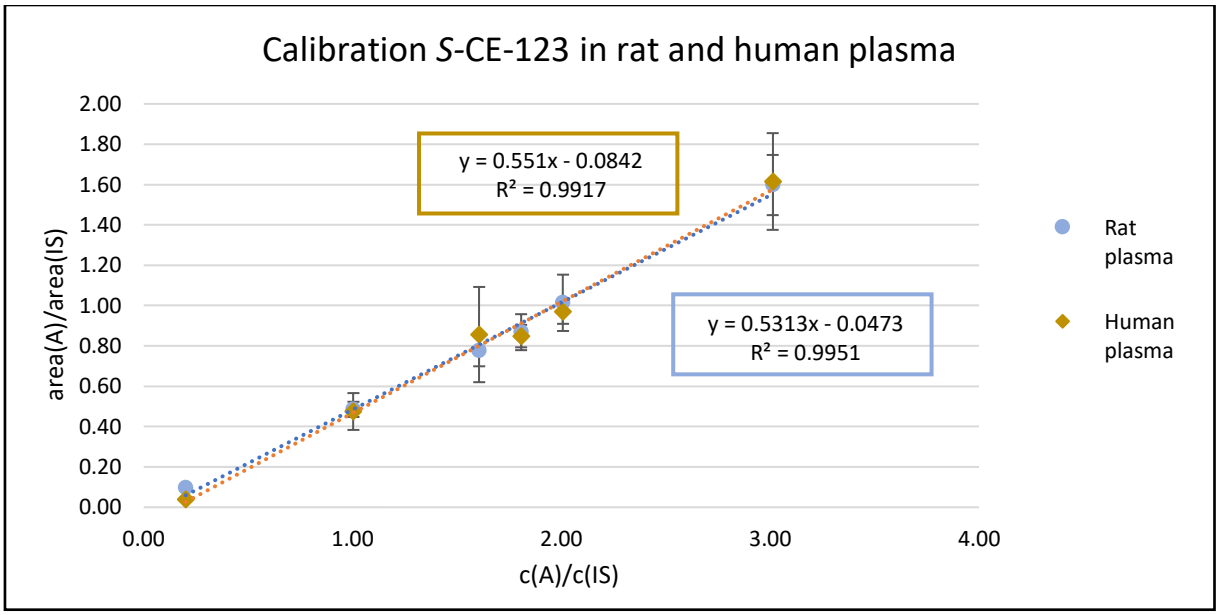

Figure 20. Calibration curve for *S*-CE-123 in the range of 100-1500 ng/mL in blank rat (blue, n = 9, ± SD) and human plasma (yellow, n = 3, ± SD). The detected area and concentration of analyte were divided by the same of IS. The individual values for rat plasma are shown in Appendix Table 5, for human plasma in Appendix Table 18. A – analyte, IS – internal standard (CE-137)

As the calibration in human plasma was not validated the differences between the calibration results could be due to differences during sample preparation. A validation could rule out this option. Other possibilities for the differences could be the composition of used plasma (e.g. plasma albumin concentration) which are not necessarily caused by species differences. Plasma protein concentrations can be influenced for example by exercise level, gender or age [46]–[48]. Hong et al. (2009) showed that the concentration of albumin greatly influenced the level of free phenytoin [49]. As mentioned before the plasma bound fraction of the drug cannot bind to any targets nor get accessed by metabolising enzymes. It is possible that the drug partly gets precipitated with the plasma protein when adding ACN or MeOH during sample preparation. Another reason could be the complete flushing of the LC-MS between the measurements for the rat plasma and the human plasma calibration. This was done in course of trouble shooting due to re-occurring errors of HR-MS while measuring batches.
Due to the incomparability and even though the human plasma calibration was not validated, the incubated human plasma samples were quantified with the calibration done in the same species.

3.5.2. Plasma curve

For the optimal comparability, the incubation experiment in human plasma was done according to the incubation experiment protocol for rat plasma (section 3.3.2). Samples spiked with 2000 ng/mL *R*-MO were incubated at 37 °C for 0.00, 0.75, 1.50, 2.25, 3.00, 4.00, 5.00, 6.00 and 8.00 h. The reaction was stopped by adding MeST. *S*-CE-123 was incubated with the concentration of 1000 ng/mL for 0.00, 2.00, 4.00, 6.00 and 8.00 h.

R-MO and MA concentrations were calculated and referred to the recovered *R*-MO concentration at t = 0.00 h to receive degradation and formation percentages respectively. *S*-CE-123 concentrations were referred to recovered *S*-CE-123 concentration at t = 0.00 h.

Even though the calibration in human plasma was not validated, the calculation of c(analyte)/c(IS) was done with the respective linear equation for each substance. As there was no markable degradation of neither of the substances and both precision and accuracy were satisfactory in the concentration range (around 2000 ng/mL for *R*-MO and 1000 ng/mL for *S*-CE-123), this was acceptable for this purpose.

Figure 21 compares the recovered *in vitro* *R*-MO and MA levels in rat and human plasma over 8 h. As previously described, in rat plasma more than 93% of *R*-MO (dark green) got metabolised and nearly 79% of the initial *R*-MO concentration were recovered as MA (light green). However, there was no significant degradation process noted in incubated human plasma samples (blue). The varying *R*-MO percentages of the human plasma samples could be explained by slight inhomogeneities of used plasma or disruptive elements for ionisation of the MS.

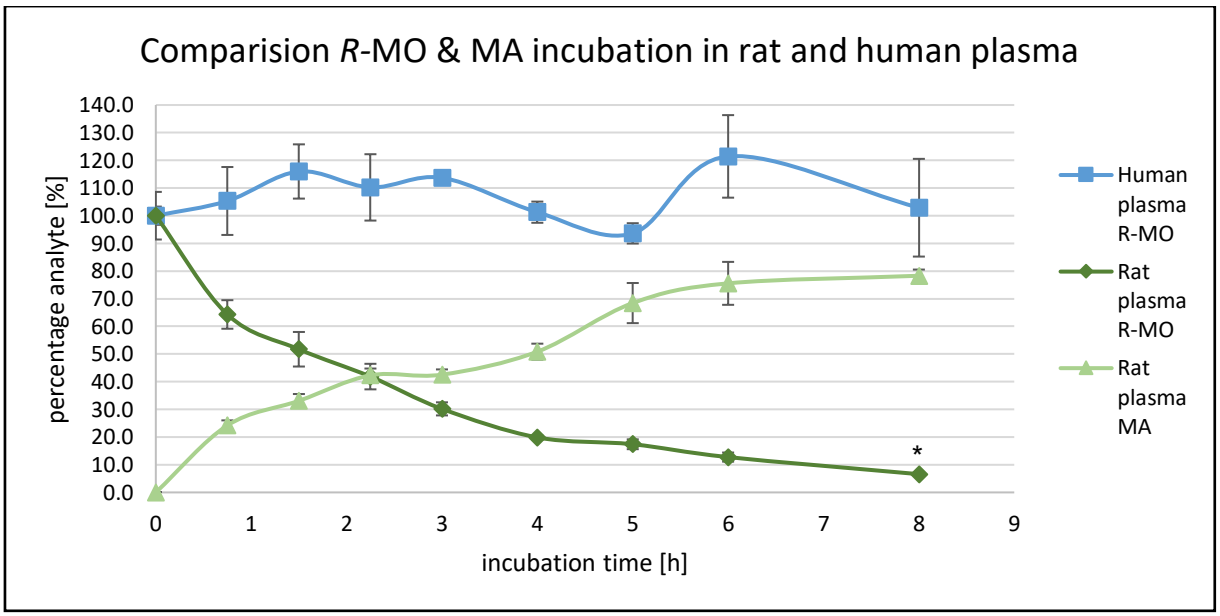

Figure 21. Comparison of the incubation *R*-MO and the formation of MA in rat and human plasma at 37 °C over 8 h (n = 3, average ± SD). The dark green plasma curve shows the degradation of *R*-MO and the light green the formation of MA in rat plasma. The percentage of formed MA was received by referring the recovered concentration of MA to the recovered *R*-MO concentration at t = 0 h. The recovered *R*-MO of human plasma samples is shown by the blue plasma curve. * Concentration could be detected but not quantified. The individual values for rat plasma *R*-MO are shown in Appendix Table 6, for rat plasma MA in Appendix Table 7 and for human plasma *R*-MO in Appendix Table 19. *R*-MO – *R*-modafinil, MA – modafinil acid

There are multiple possible reasons to explain the enhanced *in vitro* plasma stability of *R*-MO in human plasma. Firstly, a lower concentration or lower activity of the metabolising enzyme could lead to slower and not detectable degradation within the 8 hours experiment. The total absence of the metabolising enzyme in human plasma, which occurs in rat plasma, is also possible. Another explanation could be differences in plasma protein concentration of used plasma. As described before, plasma protein-bound *R*-MO cannot be metabolised by plasma enzymes.
Darwish *et al*. (2009) found that the *in vivo* elimination half-life of *R*-MO in humans is around 15 h, which is already longer than the duration of this experiment [7]. Furthermore, *in vitro* plasma studies can only look at the activity of plasma enzymes, whereas *in vivo* studies examine the effects of the eternity of metabolising enzymes – i.e. multiple different degradation routes.

Various studies have described the *in vivo* as well as the *in vitro* hepatic/microsome elimination of *R*-MO [4], [7], [8], [10], very few the *in vitro* stability in plasma. One of them, contrary to the results of this study, detected the metabolisation of *R*-MO to MA in human plasma at room temperature after 24 h [50].

The comparison of the incubation of *S*-CE-123 in rat (green) and human plasma (blue) is shown in Figure 22. As expected, there was also no *S*-CE-123 metabolisation in human plasma.

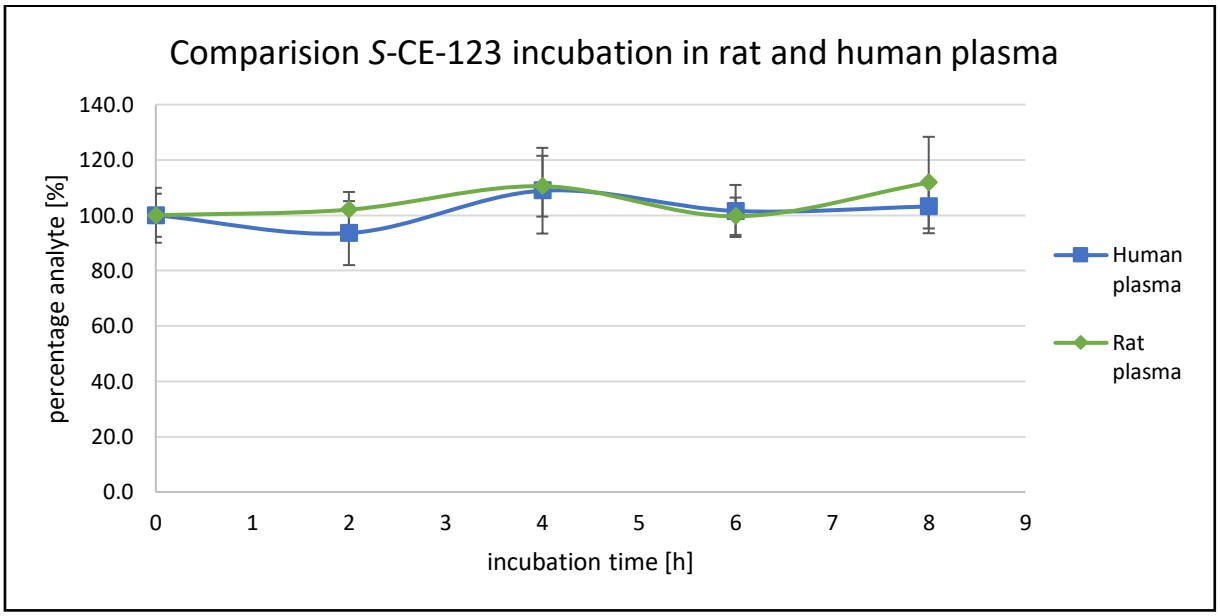

Figure 22. Comparison of recovered *S*-CE-123 following incubation in rat (green, n = 3, average ± SD) and human plasma (blue, n = 4, average ± SD) 37 °C over 8 h. The recovered concentrations of the incubated samples were referred to the respective recovered concentration at t = 0 h and plotted against the incubation time. The individual values for the incubation in rat plasma are shown in Appendix Table 8 and for human plasma in Appendix Table 20. *R*-MO – *R*-modafinil

3.6. Lipophilicity *via* logP_{ow}

Three *R*-MO and *S*-CE-123 samples were prepared, measured in triplicate and analysed to receive the Rt of analytes and the two standard substances. The Rt-values and the log P_{ow} values of standard substances from literature were used to calculate log P_{ow} of *R*-MO and *S*-CE-123 using Equation 1 [43].

Figure 23 compares the experimental established log P_{ow} -values for *R*-MO (0.989±0.018) and *S*-CE-123 (1.57±0.064) to the theoretically calculated values done by ACD/ChemSketch (1.17±0.49 and 1.81±0.50, respectively). The variation of experimental and theoretical values strongly depends on the source of the latter, as different calculation methods lead to variating results. Various databases were checked for the respective theoretical log P_{ow}-values, e.g. SciFinder, BIOVIA Draw, ACD/ChemSketch and swissadme.com (calculates the theoretical value with five different methods, iLOGP, XLOGP3, WLOGP, MLOGP, SILICO-IT). ACD/ChemSketch has shown to be the closest fit to the experimental values.

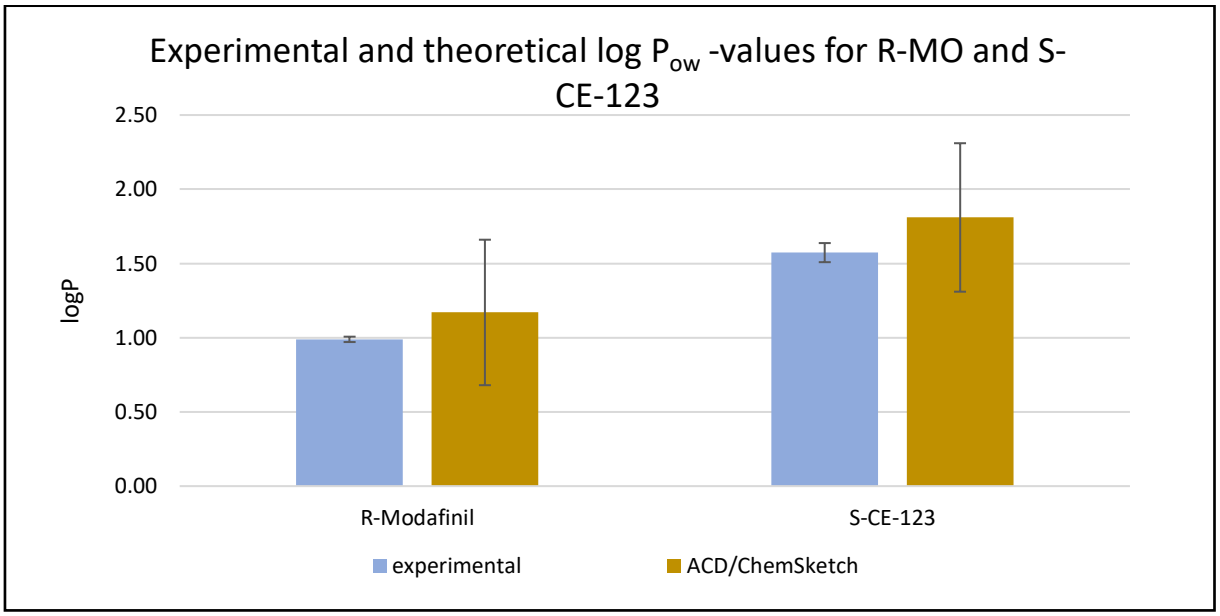

Figure 23. Results of log P_{ow} calculations for *R*-MO and *S*-CE-123 (n = 9, average ± SD) compared to the theoretically calculated log P_{ow} -values by ACD/ChemSketch (sourced on 27.06.2022). The exact retention time-values used for calculation are shown in Appendix Table 21 for *R*-MO and Appendix Table 22 for *S*-CE-123.

The differences between experimental and theoretical values can be explained by the absence of connectivity and non-bonded intramolecular interaction patterns in used databases [36].

According to the adapted 'Lipinski's rule of five', neither *R*-MO nor *S*-CE-123 would be able to penetrate the BBB, as log P_{ow} -values lie below the range of 2.0-3.5 [36]. It should be noted that measured log P_{ow} -values can differ depending on the used method. On the contrary, *R*-MO and *S*-CE-123 *in vivo* studies showed that both substances can cross the BBB [17], [19], [51]. This suggests, that the Ro5 is not completely reliable to make predictions about BBB penetration and leaves no indication of log P_{ow} threshold for passive diffusion *via* BBB. The same assumption was also done by Giménez *et al*. (2010). They evaluated the Ro5 by looking at the log P_{ow} values of blockbuster drugs (e.g. atorvastatin) and found that Ro5 could lead to exclusion of potential hits during drug discovery [52].

4. Conclusion and outlook

The *in vitro* plasma stability experiments, there was clear evidence for metabolisation processes of *R*-MO in rat plasma as only 6.6±0.5% remained after 8 h incubation. 78.3±2.2% of the initial *R*-MO concentration was metabolised to MA. The elimination half time of *R*-MO in rat plasma was determined as 1.5 h. Those degradation processes could be slowed down by adding of enzyme inhibiting substances to the rat plasma. The addition of 10% DMF lead to 66.8±7.2% remaining *R*-MO and 0.25% NaF to 53.5±4.2% remaining *R*-MO. There was no significant metabolisation detected in human plasma. These results confirm the statement done by Hale *et al.* (2000), that the plasma stability can differ in various species [27]. Reasons for this could be the absence or decreased activity of the respective amid esterase in human plasma. These two hypotheses could be proved in future experiments by identifying the responsible enzymes in rat plasma, checking for occurrence in human plasma and comparing the levels of activity in both plasma types.
S-CE-123 showed no metabolisation in neither rat nor human plasma. This can be explained by the structural differences to its parent compound and coherently decreased vulnerability to the degradation by plasma enzymes.

By validating this method, it was proven that the analytes could reliably be detected within certain concentration ranges – for *R*-MO between 200-4000 ng/mL initial concentration, MA between 200-3000 ng/mL and *S*-CE-123 between 100-1500 ng/mL. Validation was conducted according to ICH Guidelines M10 for bioanalytical methods (2019) and between-run precision and accuracy met the requirements. Results were within ± 15% and ± 20% LLOQ. As the sample preparation includes some dilution steps, the actually measured concentration was 20-times lower than the initial concentration. If it is necessary to measure lower initial analyte concentrations, dilution steps in the sample preparation could be reduced.

The determination of $\log P_{ow}$-values according to the SOP by Maisetschläger (2021)[42] resulted in 0.989±0.018 for *R*-MO and 1.57±0.064 for *S*-CE-123. The best fit of theoretical values was found to be with ACD/ChemSketch (1.17±0.49 and 1.81±0.50, respectively). Other databases calculated higher values. It has to be noted that experimental $\log P_{ow}$-values depend highly on the used determination method (i.e. used column and mobile phase)[35]. Thus, further measurements with other methods could verify these results.

To summarise all these studies, *S*-CE-123 was found to be superior to its parent compound regarding the duration of action and thus, decreased intake frequencies. The higher $\log P_{ow}$-value indicates an improved BBB passage compared to *R*-MO.

5. References

[1] ‘Ph.Eu. Modafinil Kommentar’, *Ph. Eur. 5.6, 2307 (01/2007)*.

[2] M. J. Minzenberg and C. S. Carter, ‘Modafinil: A review of neurochemical actions and effects on cognition’, *Neuropsychopharmacology*, vol. 33, no. 7. pp. 1477–1502, Jun. 2008. doi: 10.1038/sj.npp.1301534.

[3] ‘Fachinformation Modafinl Aristo 100 mg stand 07.04.2022’.

[4] Y. N. Wong *et al.*, ‘Open-label, single-dose pharmacokinetic study of modafinil tablets: influence of age and gender in normal subjects.’, *J Clin Pharmacol*, vol. 39, no. 3, pp. 281–8, Mar. 1999, [Online]. Available: http://www.ncbi.nlm.nih.gov/pubmed/10073328

[5] Y. N. Wong, S. P. King, W. B. Laughton, G. C. McCormick, and P. E. Grebow, ‘Single-dose pharmacokinetics of modafinil and methylphenidate given alone or in combination in healthy male volunteers.’, *J Clin Pharmacol*, vol. 38, no. 3, pp. 276–82, Mar. 1998, doi: 10.1002/j.1552-4604.1998.tb04425.x.

[6] S. v. Mahler *et al.*, ‘Modafinil attenuates reinstatement of cocaine seeking: Role for cystine-glutamate exchange and metabotropic glutamate receptors’, *Addiction Biology*, vol. 19, no. 1, pp. 49–60, Jan. 2014, doi: 10.1111/j.1369-1600.2012.00506.x.

[7] M. Darwish, M. Kirby, E. T. Hellriegel, R. Yang, and P. Robertson, ‘Pharmacokinetic profile of armodafinil in healthy subjects: pooled analysis of data from three randomized studies.’, *Clin Drug Investig*, vol. 29, no. 2, pp. 87–100, 2009, doi: 10.2165/0044011-200929020-00003.

[8] P. Robertson and E. T. Hellriegel, ‘Clinical pharmacokinetic profile of modafinil.’, *Clin Pharmacokinet*, vol. 42, no. 2, pp. 123–37, 2003, doi: 10.2165/00003088-200342020-00002.

[9] ‘Österreichischer Arzneispezialitätenregister Modafinil’. https://aspregister.basg.gv.at/aspregister/faces/aspregister.jspx (accessed Apr. 07, 2022).

[10] K. H. Wu *et al.*, ‘Population pharmacokinetics of modafinil acid and estimation of the metabolic conversion of modafinil into modafinil acid in 5 major ethnic groups of China’, *Acta Pharmacol Sin*, vol. 33, no. 11, pp. 1401–1408, Nov. 2012, doi: 10.1038/aps.2012.124.

[11] K. P. Garnock-Jones, S. Dhillon, and L. J. Scott, ‘Armodafinil.’, *CNS Drugs*, vol. 23, no. 9, pp. 793–803, Sep. 2009, doi: 10.2165/11203290-000000000-00000.

[12] M. Darwish, M. Kirby, P. Robertson, and E. T. Hellriegel, ‘Interaction profile of armodafinil with medications metabolized by cytochrome P450 enzymes 1A2, 3A4 and 2C19 in healthy subjects.’, *Clin Pharmacokinet*, vol. 47, no. 1, pp. 61–74, 2008, doi: 10.2165/00003088-200847010-00006.

[13] ‘Ph.Eu. Modafinil Monographie’, *Ph. Eur. 5.6, 2307 (01/2007)*.

[14] Y. N. Wong *et al.*, ‘A double-blind, placebo-controlled, ascending-dose evaluation of the pharmacokinetics and tolerability of modafinil tablets in healthy male volunteers.’, *J Clin Pharmacol*, vol. 39, no. 1, pp. 30–40, Jan. 1999, doi: 10.1177/00912709922007534.

[15] K. J. McClellan and C. M. Spencer, ‘Modafinil’, *CNS Drugs*, vol. 9, no. 4, pp. 311–324, 1998, doi: 10.2165/00023210-199809040-00006.

[16] P. Kalaba *et al.*, ‘Heterocyclic Analogues of Modafinil as Novel, Atypical Dopamine Transporter Inhibitors’, *J Med Chem*, vol. 60, no. 22, pp. 9330–9348, Nov. 2017, doi: 10.1021/acs.jmedchem.7b01313.

[17] M. Kristofova *et al.*, ‘A daily single dose of a novel modafinil analogue CE-123 improves memory acquisition and memory retrieval’, *Behavioural Brain Research*, vol. 343, pp. 83–94, May 2018, doi: 10.1016/j.bbr.2018.01.032.

[18] P. Grochecki *et al.*, 'Novel Dopamine Transporter Inhibitor, CE-123, Ameliorates Spatial Memory Deficits Induced by Maternal Separation in Adolescent Rats: Impact of Sex', *Int J Mol Sci*, vol. 23, no. 18, Sep. 2022, doi: 10.3390/ijms231810718.
[19] I. Gyertyán *et al.*, 'Cognitive profiling and proteomic analysis of the modafinil analogue S-CE-123 in experienced aged rats', *Sci Rep*, vol. 11, no. 1, Dec. 2021, doi: 10.1038/s41598-021-03372-y.
[20] P. Kalaba *et al.*, 'Structure-Activity Relationships of Novel Thiazole-Based Modafinil Analogues Acting at Monoamine Transporters', *J Med Chem*, vol. 63, no. 1, pp. 391–417, Jan. 2020, doi: 10.1021/acs.jmedchem.9b01938.
[21] A. Nikiforuk *et al.*, 'A novel dopamine transporter inhibitor CE-123 improves cognitive flexibility and maintains impulsivity in healthy male rats', *Front Behav Neurosci*, vol. 11, Nov. 2017, doi: 10.3389/fnbeh.2017.00222.
[22] L. Di and E. H. Kerns, 'Solution stability--plasma, gastrointestinal, bioassay.', *Curr Drug Metab*, vol. 9, no. 9, pp. 860–8, Nov. 2008, doi: 10.2174/138920008786485218.
[23] G. A. Reed, 'Stability of drugs, drug candidates, and metabolites in blood and plasma', *Curr Protoc Pharmacol*, vol. 2016, pp. 7.6.1-7.6.12, Dec. 2016, doi: 10.1002/cpph.16.
[24] W. E. Lindup and M. C. Orme, 'Clinical pharmacology: plasma protein binding of drugs.', *Br Med J (Clin Res Ed)*, vol. 282, no. 6259, pp. 212–4, Jan. 1981, doi: 10.1136/bmj.282.6259.212.
[25] J. Østergaard and C. Larsen, 'Bioreversible Derivatives of Phenol. 1. The Role of Human Serum Albumin as Related to the Stability and Binding Properties of Carbonate Esters with Fatty Acid-like Structures in Aqueous Solution and Biological Media', *Molecules*, vol. 12, pp. 2380–2395, 2007, [Online]. Available: www.mdpi.org/molecules
[26] M. L. Howard, J. J. Hill, G. R. Galluppi, and M. A. Mclean, 'Plasma Protein Binding in Drug Discovery and Development', 2010.
[27] J. J. Hale *et al.*, 'Phosphorylated morpholine acetal human neurokinin-1 receptor antagonists as water-soluble prodrugs', *J Med Chem*, vol. 43, no. 6, pp. 1234–1241, Mar. 2000, doi: 10.1021/jm990617v.
[28] I. Papoutsis *et al.*, 'Stability of morphine, codeine, and 6-acetylmorphine in blood at different sampling and storage conditions.', *J Forensic Sci*, vol. 59, no. 2, pp. 550–4, Mar. 2014, doi: 10.1111/1556-4029.12337.
[29] C. J. Briscoe and D. S. Hage, 'Factors affecting the stability of drugs and drug metabolites in biological matrices', *Bioanalysis*, vol. 1, no. 1. Future Science Ltd, pp. 205–220, 2009. doi: 10.4155/bio.09.20.
[30] J. Chen and Y. Hsieh, 'Stabilizing drug molecules in biological samples.', *Ther Drug Monit*, vol. 27, no. 5, pp. 617–24, Oct. 2005, doi: 10.1097/01.ftd.0000170879.18139.40.
[31] K. B. Scheidweiler, J. Shojaie, M. A. Plessinger, R. W. Wood, and T. C. Kwong, 'Stability of Methylecgonidine and Ecgonidine in Sheep Plasma in Vitro', 2000. [Online]. Available: https://academic.oup.com/clinchem/article/46/11/1787/5641168
[32] L. Di, E. H. Kerns, Y. Hong, and H. Chen, 'Development and application of high throughput plasma stability assay for drug discovery', *Int J Pharm*, vol. 297, no. 1–2, pp. 110–119, Jun. 2005, doi: 10.1016/j.ijpharm.2005.03.022.
[33] S. H. Gorman, 'Determination of modafinil, modafinil acid and modafinil sulfone in human plasma utilizing liquid-liquid extraction and high-performance liquid chromatography.', *J Chromatogr B Analyt Technol Biomed Life Sci*, vol. 767, no. 2, pp. 269–76, Feb. 2002, doi: 10.1016/s1570-0232(01)00572-4.
[34] D. Sesinova, 'Simultaneous Quantification of Modafinil, its main metabolite Modafinil acid and the novel analogCE-123in rat plasma by LC-HRMS', University of Vienna, Vienna, 2020.

[35] J. M. Pallicer, S. Pous-Torres, J. Sales, M. Rosés, C. Ràfols, and E. Bosch, 'Determination of the hydrophobicity of organic compounds measured as logPo/w through a new chromatographic method', *J Chromatogr A*, vol. 1217, no. 18, pp. 3026–3037, Apr. 2010, doi: 10.1016/j.chroma.2010.02.051.

[36] C. Vraka, L. Nics, K. H. Wagner, M. Hacker, W. Wadsak, and M. Mitterhauser, 'LogP, a yesterday's value?', *Nucl Med Biol*, vol. 50, pp. 1–10, Jul. 2017, doi: 10.1016/j.nucmedbio.2017.03.003.

[37] X. Subirats, M. Rosés, and E. Bosch, 'High-throughput log Po/w determination from UHPLC measurements: Revisiting the chromatographic hydrophobicity index', *J Pharm Biomed Anal*, vol. 127, pp. 26–31, Aug. 2016, doi: 10.1016/j.jpba.2015.12.015.

[38] Yuri. Kazakevich and Rosario. LoBrutto, *HPLC for pharmaceutical scientists*. Wiley-Interscience, 2007.

[39] T. B. Strasser, 'Method development and validation for sensitive quantification of Modafinil and ists derivative Ce-123 in PBS-diluted rat blood plasma via HPLC-HRMS', University of Vienna, Vienna, 2020.

[40] European Medicines Agency, *ICH guideline M10 on bioanalytical method validation*. 2019. [Online]. Available: www.ema.europa.eu/contact

[41] 'Merck Millipore - Sodium fluoride', *https://www.merckmillipore.com/AT/de/product/Sodium-fluoride,MDA_CHEM-106441*, Nov. 13, 2022.

[42] V. Maisetschläger, 'SOP development and standardization of preclinical HPLC methods investigating purity, lipophilicity and stability', University of Vienna, Vienna, 2021.

[43] S. F. Donovan and M. C. Pescatore, 'Method for measuring the logarithm of the octanol-water partition coefficient by using short octadecyl-poly(vinyl alcohol) high-performance liquid chromatography columns.', *J Chromatogr A*, vol. 952, no. 1–2, pp. 47–61, Apr. 2002, doi: 10.1016/s0021-9673(02)00064-x.

[44] G. Moachon and D. Matinier, 'Simultaneous determination of modafinil and its acid metabolite by high-performance liquid chromatography in human plasma.', *J Chromatogr B Biomed Appl*, vol. 654, no. 1, pp. 91–6, Mar. 1994, doi: 10.1016/0378-4347(93)e0452-v.

[45] S. R. Saroja *et al.*, 'A novel heterocyclic compound targeting the dopamine transporter improves performance in the radial arm maze and modulates dopamine receptors D1-D3', *Behavioural Brain Research*, vol. 312, pp. 127–137, Oct. 2016, doi: 10.1016/j.bbr.2016.06.011.

[46] B. G. Giménez, M. S. Santos, M. Ferrarini, and J. P. dos Santos Fernandes, 'Evaluation of blockbuster drugs under the rule-of-five', *Pharmazie*, vol. 65, no. 2, pp. 148–152, Feb. 2010, doi: 10.1691/ph.2010.9733.

6. Appendix

Appendix Table 1. Screening Experiment 1 to determine interesting time frame for the incubation of *R*-MO and *S*-CE-123 in rat plasma. Samples were prepared in duplicate and each measured in duplicate. Average [%] and SD [%] of *R*-MO and MA was all refer to the average value of *R*-MO at 0 h. The average [%] and SD [%] of *S*-CE-123 refers to the average value of *S*-CE-123 at 0 h.* S/N-ratio was below LOQ. The grey marked value was set as outliner and excluded from further calculations. *R*-MO – *R*-modafinil, MA – modafinil acid, IS – internal standard, n.d. - not detectable, SD - standard deviation, Var – variance

	t [h]	area(analyte)/area(IS)								
		A_1	A_2	B_1	B_2	Average	Average [%]	SD	SD [%]	Var [%]
***R*-MO**	0	0.28983	0.32669	0.34232	0.36613	0.33124	100.0	0.03202	9.67	9.7
	9	*0.01986	*0.02135	*0.03094	*0.02732	0.02487	7.5	0.00518	1.56	20.8
	18	n.d.	n.d.	n.d.	n.d.					
MA	0	n.d.	n.d.	n.d.	n.d.					
	9	0.06269	0.07318	0.09885	0.11011	0.08621	26.0	0.02202	6.65	25.5
	18	0.10044	0.10035	0.29989	0.14183	0.11421	34.5	0.02392	7.22	21.0
***S*-CE-123**	0	0.56535	0.55435	0.61513	0.57099	0.57645	100.0	0.02669	4.63	4.6
	9	0.64679	0.69877	0.41798	0.43271	0.54906	95.23	0.14455	25.08	26.3
	18	0.54738	0.52008	0.29795	0.28800	0.41335	71.2	0.13950	24.20	33.8

Appendix Table 2. Screening Experiment 2 to determine appropriate purification method and *S*-CE-123 degradation in rat plasma over 24 hours. Samples prepared and measured in duplicate on two different days, outliners were excluded from further calculations (n=3, apart from two values - marked grey - where only two of the four measurements could be analysed). * S/N ratio was below LOQ. *R*-MO - *R*-modafinil, MA - modafinil acid, IS - internal standard, n.d. - not detectable, SD - standard deviation, Var - variance

	t [h]	area(analyte)/area(IS)							
		PP				SPE			
		Average	SD	Var [%]	Recovery [%]	Average	SD	Var [%]	Recovery [%]
***R*-MO**	0	1.10830	0.05832	5.3	100.00	1.58030	0.099992	6.3	100.00
	4	0.25323	0.03336	13.2	22.85	0.370563	0.03918	10.6	23.45
	8	0.13385	0.02481	18.5	12.08	0.103979	0.001993	1.9	6.58
MA	0	n.d.				n.d.			
	4	0.14249	0.03303	23.2	61.15	0.175163	0.006619	3.8	63.55
	8	0.23303	0.01879	8.1	100.00	0.275641	0.021288	7.7	100.00

***S*-CE-123**	0	0.83600	0.14708	17.6	100.00	1.12520	0.038006	3.4	100.00
	4	0.61638	0.06436	10.44	73.73	1.230006	0.041029	3.3	109.31
	8	0.43725	0.05881	13.45	52.30	1.203538	0.169307	14.1	106.96
	24	0.33033	0.03338	10.11	39.51				

Appendix Table 3. Results of the *R*-MO calibration in blank rat plasma in the range of 100-4000 ng/mL. Each standard was prepared twice and measured in duplicate. The detected areas of *R*-MO peaks were divided by the detected area of IS peaks (CE-137). The lowest standard (100.6 ng/mL) had to be excluded from further analysation since the calculated S/N ratios were below LOQ. The average of each standard was converted to c(A)/c(IS) and then multiplied by the concentration of IS (500 ng/mL). Validation was carried out by repeating the protocol three times on different days, whereas some of the samples were measured a second time. Precision and accuracy were calculated, values not complying to ICH guidelines (± 15% and ± 20% at LLOQ) are marked dark grey. *R*-MO – *R*-modafinil, n – count, SD – standard deviation, c – concentration, A – analyte, IS – internal standard, n.d. – not detected

STD No.	**target conc. [ng/mL]**	**c(A)/c(IS)**	**area(*R*-MO)/area(CE-137)**						**Precision**	**Accuracy/Recovery**		
						n	Average	SD	[%]	c(A)/c(IS)	c [ng/mL]	[%]
1	100.6	0.2012	0.107975	0.074936	0.092358	9	0.081477	0.014181	17	0.4221	211.1	+ 110
			0.074684	0.063797	0.095357							
			0.068943	0.079523	0.075721							
2	201.2	0.4024	0.122697	0.140248	0.141401	10	0.130628	0.019268	15	0.5768	288.4	+ 43
			0.099680	0.098482	0.149341							
			0.123191	0.147927	0.133568							
			0.149741									
3	503.0	1.006	0.318415	0.253161	0.239785	11	0.286995	0.034437	12	1.069	534.6	+ 6
			0.287361	0.258031	0.305560							
			0.283743	0.279895	0.256516							
			0.325499	0.348978								
4	1006.0	2.012	0.509313	0.535141	0.580243	11	0.582095	0.076060	13	1.998	999.1	- 1
			0.514403	0.473475	0.681716							
			0.570683	0.542894	0.690640							
			0.633000	0.671542								
5	2012.0	4.024	1.136958	1.023483	1.142195	10	1.106582	0.056006	5	3.649	1824.6	- 9
			1.058947	1.057895	1.132870							
			1.148211	1.110368	1.052658							
			1.202229									

6	3018.0	6.036	1.531119	1.563715	1.895523	12	1.835329	0.211494	12	5.943	2971.7	- 2
			2.133214	1.754846	1.635220							
			2.200284	1.817040	1.721880							
			1.988408	1.964576	1.818122							
7	4024.0	8.048	1.948129	2.331712	2.215784	12	2.581250	0.308055	12	8.292	4145.8	- 3
			2.940748	2.916649	2.731365							
			2.905019	2.723765	2.377362							
			2.696991	2.629246	2.558233							

Appendix Table 4. Results of the MA calibration in blank rat plasma in the range of 200-3000 ng/mL. Each standard was prepared twice and measured in duplicate. The detected areas of MA peaks were divided by the detected area of IS peaks (CE-137). The average of each standard was converted to c(A)/c(IS) and then multiplied by the concentration of IS (500 ng/mL). Validation was carried out by repeating the protocol three times on different days, whereas some of the samples were measured a second time. Due to technical issues the average of STD 7 was calculated with eight values. Precision and accuracy were calculated, values not complying to ICH guidelines (± 15% and ± 20% at LLOQ) are marked dark grey. MA – modafinil acid, n – count, SD – standard deviation, c – concentration, A – analyte, IS – internal standard, n.d. – not detected

STD No.	**target conc. [ng/mL]**	**c(A)/c(IS)**	**area(MA)/area(CE-137)**						**Precision**	**Accuracy/Recovery**		
						n	Average	SD	[%]	c(A)/c(IS)	c [ng/mL]	[%]
1	200.8	0.4016	0.050170	0.036343	0.038254	11	0.036168	0.006995	19	0.5346	267.3	+ 33
			0.045155	0.037041	0.025703							
			0.038393	0.031261	0.034731							
			0.030093	0.030709								
2	502	1.004	0.087132	0.097065	0.070368	11	0.086153	0.010943	13	1.178	588.9	+ 17
			0.075473	0.078737	0.083761							
			0.100604	0.076334	0.081648							
			0.094166	0.102393								
3	803.2	1.606	0.095573	0.125581	0.100454	9	0.114230	0.015585	14	1.539	769.6	- 4
			0.102016	0.109743	0.112168							
			0.119151	0.116384	0.147001							
4	1204.8	2.410	0.149879	0.184677	0.183139	11	0.162414	0.023460	14	2.159	1079.6	- 10
			0.168121	0.135811	0.155617							
			0.119269	0.151451	0.201723							
			0.172660	0.164204								

5	1606.4	3.213	0.200592	0.207862	0.237881	11	0.245389	0.034589	14	3.227	1613.5	0
			0.266261	0.246830	0.311469							
			0.239934	0.298101	0.223914							
			0.241033	0.225400								
6	2008	4.016	0.261080	0.278585	0.297612	9	0.288939	0.032065	11	3.787	1893.7	- 6
			0.255930	0.362894	0.292677							
			0.280405	0.302943	0.268324							
7	3012	6.024	0.469078	0.508834	0.508834	8	0.480225	0.065706	14	6.249	3124.5	+ 4
			0.403434	0.420003	0.538724							
			0.409882	0.583013								

Appendix Table 5. Results of the *S*-CE-123 calibration in blank rat plasma in the range of 100-1500 ng/mL. Each standard was prepared twice and measured in duplicate. The detected areas of *S*-CE-123 peaks were divided by the detected area of IS peaks (CE-137). The average of each standard was converted to c(A)/c(IS) and then multiplied by the concentration of IS (500 ng/mL). Validation was carried out by repeating the protocol three times on different days, whereas some of the samples were measured a second time. Precision and accuracy were calculated, values not complying to ICH guidelines (± 15% and ± 20% at LLOQ) are marked dark grey. n – count, stdev – standard deviation, c – concentration, A – analyte, IS – internal standard, n.d. – not detected

STD No.	**target conc. [ng/mL]**	**c(A)/c(IS)**	**area(CE-123)/area(CE-137)**						**Precision**	**Accuracy/Recovery**		
						n	Average	SD	[%]	c(A)/c(IS)	c [ng/mL]	[%]
1	100.4	0.2008	0.095059	0.082938	0.081594	11	0.096425	0.014075	15	0.2705	135.2	+ 35
			0.107140	0.113474	0.084012							
			0.092896	0.082086	0.114526							
			0.089828	0.117126								
2	502.0	1.004	0.537938	0.471382	0.467676	12	0.485369	0.037598	8	1.003	501.3	0
			0.492005	0.518289	0.477832							
			0.511426	0.498382	0.413412							
			0.509130	0.505571	0.421385							
3	803.2	1.606	0.713318	0.756325	0.758830	11	0.775665	0.076628	10	1.549	774.5	- 4
			0.700185	0.711061	0.711120							
			0.955430	0.764948	0.820296							
			0.791141	0.849661								

4	903.6	1.807	0.815751	0.935605	0.785219	11	0.868227	0.089200	10	1.723	861.6	- 5
			0.968990	0.973437	0.735461							
			0.810585	0.808716	0.825895							
			0.890835	1.000005								
5	1004.0	2.008	1.337215	1.036363	0.868918	12	1.013699	0.139688	14	1.997	998.5	- 1
			0.869762	1.159115	1.110234							
			0.931547	0.943123	0.930605							
			1.099208	0.927808	0.950485							
6	1506.0	3.012	1.333344	1.556379	1.607564	11	1.597681	0.149207	9	3.096	1548.1	+ 3
			1.442315	1.515935	1.807875							
			1.675883	1.813403	1.535550							
			1.555638	1.730603								

Appendix Table 6. Results of the incubation of *R*-MO in rat plasma over 8 h. Two samples were incubated for each time (A and B) and measured in duplicate. The detected areas of *R*-MO peaks were divided by the detected area of IS peaks (CE-137). The average of the same time was converted to c(A)/c(IS) and then multiplied by the concentration of IS (500 ng/mL). The calculated concentrations were referred to the recovered *R*-MO concentration at t = 0 h to receive the degradation in percent. The samples at t = 8 h could only be detected and not quantified due to S/N ratios below LOQ (n = 3). *R*-MO – *R*-modafinil, SD – standard deviation, Var – variation coefficient, c – concentration, A – analyte, IS – internal standard, n.i. – not injected by LCMS

Incubation time [h]	**area(*R*-MO)/area(CE-137)**							**Recovery**		**[% *R*-MO]**	**SD [% *R*-MO]**
	A_1	A_2	B_1	B_2	Average	SD	Var [%]	c(A)/c(IS)	c [ng/mL]		
0	1.69907	1.38348	1.52535	1.48958	1.52437	0.13112	8.6	4.954	2477.2	100.00	8.60
0.75	1.03102	0.86506	1.02642	0.95432	0.96920	0.07781	8.0	3.186	1593.1	64.31	5.16
1.5	0.66228	0.86790	0.73349	0.83094	0.77365	0.09342	12.1	2.563	1281.7	51.74	6.25
2.25	0.60224	0.55810	0.71776	0.60201	0.62003	0.06838	11.0	2.074	1037.0	41.86	4.62
3	0.39359	0.44708	0.47645	0.43691	0.43851	0.03432	7.8	1.496	747.9	30.19	2.36
4	0.28908	0.27561	0.26600	0.28085	0.27788	0.00967	3.5	0.9842	492.1	19.87	0.69
5	0.26239	0.25723	0.21109	0.22750	0.23955	0.02442	10.2	0.8621	431.1	17.40	1.77
6	n.i.	0.15409	0.19225	0.15591	0.16741	0.02153	12.9	0.6324	316.2	12.76	1.64
8	0.06864	0.07593	0.06491	0.07598	0.07136	0.00552	7.7	0.3264	163.2	6.59	0.51

Appendix Table 7. Results of the incubation of *R*-MO and formation of MA in rat plasma over 8 h. Two samples were incubated for each time (A and B) and measured in duplicate. The detected areas of MA peaks were divided by the detected area of IS peaks (CE-137). The average of the same time was converted to c(A)/c(IS) and then multiplied by the concentration of IS (500 ng/mL). The calculated concentrations were referred to the recovered *R*-MO concentration at t = 0 h to receive the formation in percent based on *R*-MO (n = 3). MA – modafinil acid, *R*-MO – *R*-modafinil, SD – standard deviation, Var – variation coefficient, c – concentration, A – analyte, IS – internal standard, n.d. – not detected, n.i. – not injected by LCMS

Incubation time [h]	**area(MA)/area(CE-137)**							**Recovery**		**[% MA]**	**[% *R*-MO]**	**SD [% *R*-MO]**
	A_1	A_2	B_1	B_2	Average	SD	Var [%]	c(A)/c(IS)	c [ng/mL]			
0	n.d.	n.d.	n.d.	n.d.								
0.75	0.08609	n.d.	0.096477	0.0838846	0.088817	0.006725	7.6	1.199	599.5	30.91	24.20	1.83
1.5	0.112644	0.1232595	0.130698	n.d.	0.1222	0.009074	7.4	1.640	820.0	42.27	33.10	2.46
2.25	n.d.	0.1672419	0.151293	0.1517546	0.156763	0.009078	5.8	2.096	1048.2	54.04	42.32	2.45
3	0.163708	0.1593688	0.14998	n.d.	0.157686	0.007017	4.5	2.109	1054.3	54.36	42.56	1.89
4	0.17702	0.199805	0.182639	0.1957652	0.188807	0.010745	5.7	2.520	1259.9	64.96	50.86	2.89
5	n.d.	0.2321974	0.284631	0.2472211	0.254683	0.027001	10.6	3.390	1695.0	87.39	68.42	7.25
6	n.i.	0.2807135	0.252897	0.3106693	0.281427	0.028893	10.3	3.743	1871.7	96.50	75.56	7.76
8	0.286881	0.2825111	0.299973	0.2974821	0.291712	0.008357	2.9	3.879	1939.6	100.00	78.30	2.24

Appendix Table 8. Results of the incubation of *S*-CE-123 in rat plasma over 8 h. Two samples were incubated for each time (A and B) and measured in duplicate. The detected areas of *S*-CE-123 peaks were divided by the detected area of IS peaks (CE-137). The average of the same time was converted to c(A)/c(IS) and then multiplied by the concentration of IS (500 ng/mL). The calculated concentrations were referred to the recovered *S*-CE-123 concentration at t = 0 h to receive the degradation in percent. SD – standard deviation, Var – variation coefficient, c – concentration, A – analyte, IS – internal standard

Incubation time [h]	**area(CE-123)/area(CE-137)**							**Recovery**		**[% CE-123]**	**SD [% CE-123]**
	A_1	A_2	B_1	B_2	Average	SD	Var [%]	c(A)/c(IS)	c [ng/mL]		
0	1.043929	1.0127632	1.259473	1.103371	1.104884	0.109699	9.9	2.169	1084.3	100.00	9.93
2	1.081877	1.0774756	1.124384	1.2294726	1.128302	0.070686	6.3	2.213	1106.4	102.03	6.39
4	1.070469	1.1867676	1.318354	1.3276461	1.225809	0.121915	10.0	2.396	1198.1	110.50	10.99
6	1.149128	1.1266546	1.137732	0.989688	1.100801	0.074641	6.8	2.161	1080.5	99.65	6.76
8	1.082763	1.4988312	1.141888	1.2393274	1.240703	0.183795	14.8	2.424	1212.1	111.79	16.56

Appendix Table 9. Summary of detected *R*-MO and MA percentages (n = 3) after 8 h incubation. All recovered concentrations of both data sets were referred to the recovered *R*-MO concentration at t = 0 h. Individual values are shown in Appendix Table 6 for *R*-MO and Appendix Table 7 for MA. *R*-MO – *R*-modafinil, MA – modafinil acid

Incubation time [h]	% *R*-MO	% MA	% *R*-MO +% MA
0	100.00	0.00	100.00
0.75	64.31	24.20	88.51
1.5	51.74	33.10	84.84
2.25	41.86	42.32	84.18
3	30.19	42.56	72.75
4	19.87	50.86	70.73
5	17.40	68.42	85.83
6	13.73	75.56	89.28
8	6.59	78.30	84.89

Appendix Table 10. Results of the incubation of *R*-MO in DMF 10% spiked rat plasma over 8 h. Two samples were incubated for each time (A and B) and measured in duplicate. The detected areas of *R*-MO peaks were divided by the detected area of IS peaks (CE-137). The average of the same time was converted to c(A)/c(IS) and then multiplied by the concentration of IS (500 ng/mL). The calculated concentrations were referred to the recovered *R*-MO concentration at t = 0 h to receive the degradation in percent. *R*-MO – *R*-modafinil, SD – standard deviation, Var – variation coefficient, c – concentration, A – analyte, IS – internal standard

Incubation time [h]	area(*R*-MO)/area(CE-137)							Recovery		[% *R*-MO]	SD [% *R*-MO]
	A_1	A_2	B_1	B_2	Average	SD	Var [%]	c(A)/c(IS)	c [ng/mL]		
0	2.20619	2.45962	1.98744	2.12239	1.98754	0.25650	12.9	6.430	3214.8	100.00	12.91
2	1.75586	1.80721	1.78137	1.78023	1.46852	0.24491	16.7	4.777	2388.3	74.29	12.39
4	1.26253	1.35909	1.24870	1.35914	1.42303	0.21762	15.3	4.6317	2315.8	72.04	11.02
6	1.20733	1.18377	1.40961	1.46744	1.31704	0.14258	10.8	4.2940	2147.0	66.78	7.23
8	1.69565	1.71945	1.31909	1.8445726	1.64469	0.22668	13.8	5.3377	2668.8	83.02	11.44

Appendix Table 11. Results of the incubation of *R*-MO and formation of MA in DMF 10% spiked rat plasma over 8 h. Two samples were incubated for each time (A and B) and measured in duplicate. The detected areas of MA peaks were divided by the detected area of IS peaks (CE-137). The average of the same time was converted to c(A)/c(IS) and then multiplied by the concentration of IS (500 ng/mL). The calculated concentrations were referred to the recovered *R*-MO concentration at t = 0 h to receive the degradation in percent. *R*-MO – *R*-modafinil, MA – modafinil acid, SD – standard deviation, Var – variation coefficient, c – concentration, A – analyte, IS – internal standard, n.d. – not detected

Incubation time [h]	**area(MA)/area(CE-137)**							**Recovery**		**[% MA]**	**[% *R*-MO]**	**SD [% *R*-MO]**
	A_1	A_2	B_1	B_2	Average	SD	Var [%]	c(A)/c(IS)	c [ng/mL]			
0	n.d.	n.d.	n.d.	n.d.								
2	n.d.	0.0109126	n.d.	0.0138835	0.012398	0.002101	16.9	0.189	94.7	81.19	2.95	0.50
4	0.012341	0.0121767	0.008802	0.0077426	0.010266	0.002343	22.8	0.161	80.6	69.11	2.51	0.57
6	0.021318	0.0072774	0.024297	0.0096928	0.015646	0.008416	53.8	0.232	116.1	99.59	3.61	1.94
8	0.021171	0.0154893	0.013435	0.0127796	0.015719	0.003814	24.3	0.233	116.6	100.00	3.63	0.88

Appendix Table 12. Results of the incubation of *S*-CE-123 in DMF 10% spiked rat plasma over 8 h. Two samples were incubated for each time (A and B) and measured in duplicate. The detected areas of *S*-CE-123 peaks were divided by the detected area of IS peaks (CE-137). The average of the same time was converted to c(A)/c(IS) and then multiplied by the concentration of IS (500 ng/mL). The calculated concentrations were referred to the recovered *S*-CE-123 concentration at t = 0 h to receive the degradation in percent. SD – standard deviation, Var – variation coefficient, c – concentration, A – analyte, IS – internal standard

Incubation time [h]	**area(CE-123)/area(CE-137)**							**Recovery**		**[% CE-123]**	**SD [% CE123]**
	A_1	A_2	B_1	B_2	Average	SD	Var [%]	c(A)/c(IS)	c [ng/mL]		
0	0.979059	1.1909206	1.071138	1.1828934	1.106003	0.100753	9.1	2.171	1085.4	100.00	9.11
2	1.119937	1.1931884	1.032538	1.1224389	1.117026	0.065769	5.9	2.191	1095.7	100.96	5.94
4	1.066594	1.1532662	1.15891	1.2227634	1.150383	0.064137	5.6	2.254	1127.1	103.85	5.79
6	1.021405	1.107827	1.058134	1.0566771	1.061011	0.035531	3.4	2.086	1043.0	96.10	3.22
8	1.072982	1.0912266	1.11671	1.1026965	1.095904	0.018496	1.7	2.152	1075.9	99.12	1.67

Appendix Table 13. Results of the incubation of *R*-MO in NaF 0.25% spiked rat plasma over 8 h. Two samples were incubated for each time (A and B) and measured in duplicate. The detected areas of *R*-MO peaks were divided by the detected area of IS peaks (CE-137). The average of the same time was converted to c(A)/c(IS) and then multiplied by the concentration of IS (500 ng/mL). The calculated concentrations were referred to the recovered *R*-MO concentration at t = 0 h to receive the degradation in percent. *R*-MO – *R*-modafinil, SD – standard deviation, Var – variation coefficient, c – concentration, A – analyte, IS – internal standard

Incubation time [h]	**area(*R*-MO)/area(CE-137)**							**Recovery**		**[% *R*-MO]**	**SD [% *R*-MO]**
	A_1	A_2	B_1	B_2	Average	SD	Var [%]	c(A)/c(IS)	c [ng/mL]		
0	1.75320	1.75271	2.75349	2.55993	2.20483	0.52773	23.9	7.122	3560.9	100.00	23.94
2	2.01602	1.86524	1.95914	1.76813	1.90213	0.10884	5.7	6.158	3078.8	95.77	5.48
4	1.37991	1.25786	2.02211	1.70477	1.59116	0.34367	21.6	5.1672	2583.6	80.36	17.36
6	1.03864	0.94786	1.14872	1.05831	1.04838	0.08239	7.9	3.4384	1719.2	53.48	4.20
8	0.07285	0.97197	0.94260	0.95707	0.73612	0.44235	60.1	2.4438	1221.9	38.01	22.84

Appendix Table 14. Results of the incubation of *R*-MO and formation of MA in NaF 0.25% spiked rat plasma over 8 h. Two samples were incubated for each time (A and B) and measured in duplicate. The detected areas of MA peaks were divided by the detected area of IS peaks (CE-137). The average of the same time was converted to c(A)/c(IS) and then multiplied by the concentration of IS (500 ng/mL). The calculated concentrations were referred to the recovered *R*-MO concentration at t = 0 h to receive the degradation in percent. *R*-MO – *R*-modafinil, MA – modafinil acid, SD – standard deviation, Var – variation coefficient, c – concentration, A – analyte, IS – internal standard, n.d. – not detected

Incubation time [h]	**area(MA)/area(CE-137)**							**Recovery**		**[% MA]**	**[% *R*-MO]**	**SD [% *R*-MO]**
	A_1	A_2	B_1	B_2	Average	SD	Var [%]	c(A)/c(IS)	c [ng/mL]			
0	n.d.	n.d.	n.d.	n.d.								
2	0.042124	0.0360018	0.031797	0.0282185	0.034535	0.005976	17.3	0.482	240.9	206.57	7.49	1.30
4	0.023472	0.0226552	0.060663	0.0606772	0.041867	0.021715	51.9	0.579	289.3	248.10	9.00	4.67
6	0.041507	0.0409493	0.040535	0.0383312	0.040331	0.001391	3.5	0.558	279.2	239.39	8.68	0.30
8	0.050597	0.0454269	0.03978	0.0453382	0.045286	0.004418	9.8	0.624	311.9	267.46	9.70	0.95

Appendix Table 15. Results of the incubation of *S*-CE-123 in NaF 0.25% spiked rat plasma over 8 h. Two samples were incubated for each time (A and B) and measured in duplicate. The detected areas of *S*-CE-123 peaks were divided by the detected area of IS peaks (CE-137). The average of the same time was converted to c(A)/c(IS) and then multiplied by the concentration of IS (500 ng/mL). The calculated concentrations were referred to the recovered *S*-CE-123 concentration at t = 0 h to receive the degradation in percent. SD – standard deviation, Var – variation coefficient, c – concentration, A – analyte, IS – internal standard

Incubation time [h]	**area(CE-123)/area(CE-137)**							**Recovery**		**[% CE-123]**	**SD [% CE123]**
	A_1	A_2	B_1	B_2	Average	SD	Var [%]	c(A)/c(IS)	c [ng/mL]		
0	1.040581	1.0255426	1.072107	1.0243862	1.040654	0.022229	2.1	2.048	1023.9	100.00	2.14
2	1.068389	0.9950148	1.102207	1.1163982	1.070502	0.054205	5.1	2.104	1052.0	96.92	4.91
4	1.05164	1.1397424	1.061645	1.0677647	1.080198	0.040249	3.7	2.122	1061.1	97.76	3.64
6	0.997115	1.0074449	0.972162	0.98412	0.99021	0.015357	1.6	1.953	976.4	89.96	1.40
8	1.002846	0.996387	1.007694	1.036868	1.010949	0.01789	1.8	1.992	995.9	91.76	1.62

Appendix Table 16. Results of the *R*-MO calibration in human plasma in the range of 100-4000 ng/mL. Each standard was prepared twice and measured in duplicate. The detected areas of *R*-MO peaks were divided by the detected area of IS peaks (CE-137). Outliners (marked light grey) were excluded from further calculations. The average of the standard was converted to c(A)/c(IS) and then multiplied by the concentration of IS (504.5 ng/mL). This calibration was not validated, precision and accuracy were calculated within this data set. Values not complying to ICH guidelines (± 15% and ± 20% at LLOQ) are marked dark grey. *R*-MO – *R*-modafinil, n – count, SD – standard deviation, Var – variation coefficient, c – concentration, A – analyte, IS – internal standard, n.d. – not detected

STD No.	**target conc. [ng/mL]**	**c(A)/c(IS)**	**area(*R*-MO)/area(CE-137)**							**Precision**	**Accuracy/Recovery**		
							n	Average	SD	[%]	c(A)/c(IS)	true conc.	
												[ng/mL]	[%]
1	101.4	0.201	0.075645	0.121831	0.040845	0.131260	4	0.092395	0.042091	46	0.3916	197.5	+ 95
2	202.8	0.402	0.195480	0.110178	0.178716	0.081724	3	0.161458	0.045194	28	0.5190	261.8	+ 29
3	507.0	1.005	n.d.	0.396240	0.364307	0.417092	3	0.392546	0.026586	7	0.9453	476.9	- 6
4	1014.0	2.010	0.842634	0.865360	0.746825	1.050637	4	0.876364	0.127030	14	1.8379	927.2	- 9
5	2028.0	4.020	2.083256	2.369884	1.898470	1.924906	4	2.069129	0.216470	10	4.0385	2037.4	0
6	3042.0	6.030	3.625529	2.861194	2.787879	2.234062	4	2.877166	0.572089	20	5.5293	2789.5	- 8
7	4056.0	8.040	4.637325	4.875875	4.522592	4.213629	3	4.457849	0.219142	5	8.4455	4260.8	+ 5

Appendix Table 17. Results of the MA calibration in human plasma in the range of 200-4000 ng/mL. Each standard was prepared twice and measured in duplicate. The detected areas of MA peaks were divided by the detected area of IS peaks (CE-137). Outliners (marked light grey) were excluded from further calculations. The average of the standard was converted to c(A)/c(IS) and then multiplied by the concentration of IS (504.5 ng/mL). This calibration was not validated, precision and accuracy were calculated within this data set. Values not complying to ICH guidelines (± 15% and ± 20% at LLOQ) are marked dark grey. MA – modafinil acid, n – count, SD – standard deviation, c – concentration, A – analyte, IS – internal standard, n.d. – not detected

STD No.	target conc. [ng/mL]	c(A)/c(IS)	area(MA)/area(CE-137)							Precision	Accuracy/Recovery		
							n	Average	SD	[%]	c(A)/c(IS)	true conc.	
												[ng/mL]	[%]
1	201.4	0.399	n.d	n.d	n.d	n.d.							
2	503.5	0.998	0.108070	0.054428	0.085141	0.240037	3	0.082546	0.026915	33	0.868	438.1	- 13
3	805.6	1.597	n.d.	0.112974	0.124938	0.097414	3	0.111775	0.013801	12	1.436	724.7	- 10
4	1208.4	2.395	0.162603	0.081766	0.226550	0.221663	4	0.173145	0.067497	39	2.629	1326.4	+ 10
5	1611.2	3.194	0.349977	0.177820	0.183431	0.273452	3	0.211567	0.053667	25	3.376	1703.2	+ 6
6	2014.0	3.992	0.227231	0.369701	0.237971	0.264773	3	0.243325	0.019335	8	3.993	2014.5	0
7	3021.0	5.988	0.330573	0.300348	0.378192	0.348604	4	0.339429	0.032622	10	5.861	2956.9	- 2

Appendix Table 18. Results of the *S*-CE-123 calibration in human plasma in the range of 100-1500 ng/mL. Each standard was prepared twice and measured in duplicate. The detected areas of *S*-CE-123 peaks were divided by the detected area of IS peaks (CE-137). Outliners (marked light grey) were excluded from further calculations. The average of the standard was converted to c(A)/c(IS) and then multiplied by the concentration of IS (504.5 ng/mL). This calibration was not validated, precision and accuracy were calculated within this data set. Values not complying to ICH guidelines (± 15% and ± 20% at LLOQ) are marked dark grey. n – count, SD – standard deviation, c – concentration, A – analyte, IS – internal standard, n.d. – not detected

STD No.	target conc. [ng/mL]	c(A)/c(IS)	area(*S*-CE-123)/area(CE-137)							Precision	Accuracy/Recovery		
							n	Average	SD	[%]	c(A)/c(IS)	true conc.	
												[ng/mL]	[%]
1	101.3	0.201	0.135835	0.047593	0.028391	0.043875	3	0.039953	0.010184	25	0.225	113.7	+ 12
2	506.5	1.004	0.565477	0.382772	0.476223	0.278713	3	0.474824	0.091360	19	1.015	511.9	+ 1
3	810.4	1.606	n.d.	0.944904	0.588746	1.035261	3	0.856304	0.236075	27	1.707	861.1	+ 6
4	911.7	1.807	0.897656	0.860303	0.788157	0.748331	3	0.848705	0.055663	7	1.693	854.2	- 6
5	1013.0	2.008	1.034924	1.387260	0.914110	0.961854	3	0.970296	0.060848	6	1.914	965.5	- 5
6	1519.5	3.012	1.895638	1.730577	1.449434	1.385210	4	1.615215	0.239674	15	3.084	1556.0	+ 2

Appendix Table 19. Results of the incubation of *R*-MO in human plasma over 8 h. Two samples were incubated for each time (A and B) and measured in duplicate. The detected areas of *R*-MO peaks were divided by the detected area of IS peaks (CE-137). Outliners were excluded from further calculations (marked grey). The average of the same time was converted to c(A)/c(IS) and then multiplied by the concentration of IS (500 ng/mL). The calculated concentrations were referred to the recovered *R*-MO concentration at t = 0 h to receive the degradation in percent (n = 3). *R*-MO – *R*-modafinil, SD – standard deviation, Var – variation coefficient, c – concentration, A – analyte, IS – internal standard

Incubation time [h]	**area(*R*-MO)/area(CE-137)**							**Recovery**		**[% MO]**	**SD [% MO]**
	A_1	A_2	B_1	B_2	Average	SD	Var [%]	c(A)/c(IS)	c [ng/mL]		
0	1.95226	2.06362	1.94857	2.62032	1.98815	0.06539	3.3	3.889	1962.0	100.0	3.3
0.75	2.01613	1.80719	2.20083	2.37711	2.10032	0.24476	11.7	4.096	2066.4	105.3	12.3
1.5	2.26859	2.24616	2.61343	2.17251	2.32517	0.19650	8.5	4.511	2275.7	116.0	9.8
2.25	2.98076	1.96250	2.20701	2.44188	2.20380	0.23971	10.9	4.287	2162.8	110.2	12.0
3	2.26377	2.22376	2.30036	2.32104	2.27723	0.04279	1.9	4.422	2231.1	113.7	2.1
4	1.99740	1.92130	2.03715	2.10341	2.01481	0.07615	3.8	3.938	1986.9	101.3	3.8
5	3.45533	1.85339	1.78104	1.92631	1.85358	0.07263	3.9	3.641	1836.8	93.6	3.7
6	2.75211	2.56534	2.39576	2.04701	2.44006	0.29973	12.3	4.723	2382.7	121.4	14.9
8	1.97015	2.80569	1.74337	2.43334	2.04896	0.35167	17.2	4.001	2018.6	102.9	17.7

Appendix Table 20. Results of the incubation of *S*-CE-123 in human plasma over 8 h. Two samples were incubated for each time (A and B) and measured in duplicate. The detected areas of *S*-CE-123 peaks were divided by the detected area of IS peaks (CE-137). The average of the same time was converted to c(A)/c(IS) and then multiplied by the concentration of IS (500 ng/mL). The calculated concentrations were referred to the recovered *S*-CE-123 concentration at t = 0 h to receive the degradation in percent (n = 4). SD – standard deviation, Var – variation coefficient, c – concentration, A – analyte, IS – internal standard

Incubation time [h]	**area(*S*-CE-123)/area(CE-137)**							**Recovery**		**[% CE-123]**	**SD [% CE123]**
	A_1	A_2	B_1	B_2	Average	SD	Var [%]	c(A)/c(IS)	c [ng/mL]		
0	1.18090	1.08760	1.15297	1.30713	1.18215	0.09204	7.8	2.298	1159.5	100.0	7.8
2	1.27946	0.96359	1.03544	1.12377	1.10056	0.13607	12.4	2.150	1084.8	93.6	11.6
4	1.12831	1.55762	1.25647	1.23599	1.29460	0.18414	14.2	2.502	1262.4	108.9	15.5
6	1.22895	1.32490	1.19750	1.05589	1.20181	0.11135	9.3	2.334	1177.5	101.6	9.4
8	1.07384	1.27856	1.19843	1.33818	1.22225	0.11431	9.4	2.371	1196.2	103.2	9.6

Appendix Table 21. Measurement and calculation results for $logP_{ow}$ determination of *R*-MO. Rt of toluene, triphenylene and *R*-MO were received by integration of the according peaks of each sample. The received Rt for *R*-MO and for toluene and triphenylene were then used to calculate $logP_{ow}$ using Equation 1. Equation 1 and the literature values $logP_{ow}$(toluene) = 2.69 and $logP_{ow}$(triphenylene) = 5.49 [43]. The theoretical value was sourced from ACD/ChemSketch on 27.06.2022. Rt – retention time, *R*-MO – *R*-modafinil, SD - standard deviation, Var – variance

Analyte	**Rt [min]**			**$logP_{ow}$ (analyte)**			
	toluene	triphenylene	analyte	Cal. $logP_{ow}$	Average	SD	Var [%]
***R*-MO 1_01**	4.380	9.173	1.506	1.011	0.999	0.016	1.6
***R*-MO 1_02**	4.364	9.054	1.501	0.981			
***R*-MO 1_03**	4.371	9.138	1.502	1.005			
***R*-MO 2_01**	4.482	9.222	1.607	0.992	0.982	0.023	2.3
***R*-MO 2_02**	4.512	9.199	1.679	0.998			
***R*-MO 2_03**	4.486	9.096	1.630	0.955			
***R*-MO 3_01**	4.513	9.093	1.757	1.005	0.986	0.017	1.7
***R*-MO 3_02**	4.477	9.072	1.663	0.975			
***R*-MO 3_03**	4.477	9.222	1.574	0.977			
				Average	0.989	0.018	1.8
				Theory	1.17	0.49	41.8

Appendix Table 22. Measurement and calculation results for $logP_{ow}$ determination of *S*-CE-123. Rt of toluene, triphenylene and *S*-CE-123 were received by integration of the according peaks of each sample. The received Rt for *S*-CE-123 and for toluene and triphenylene were then used to calculate $logP_{ow}$ using Equation 1. Equation 1 and the literature values $logP_{ow}$(toluene) = 2.69 and $logP_{ow}$(triphenylene) = 5.49 [43]. The theoretical value was sourced from ACD/ChemSketch on 27.06.2022. Rt – retention time, SD - standard deviation, Var – variance

Analyte	**Rt [min]**			**$logP_{ow}$ (analyte)**			
	toluene	triphenylene	analyte	Cal. $logP_{ow}$	Average	SD	Var [%]
CE-123 1_01	4.389	9.131	2.371	1.50	1.50	0.001	0.1
CE-123 1_02	4.395	9.142	2.377	1.50			
CE-123 1_03	4.395	9.146	2.373	1.50			
CE-123 2_01	4.526	9.575	2.689	1.67	1.61	0.057	3.5
CE-123 2_02	4.486	9.119	2.613	1.56			
CE-123 2_03	4.508	9.286	2.672	1.61			
CE-123 3_01	4.518	9.364	2.683	1.63	1.61	0.029	1.8
CE-123 3_02	4.476	9.172	2.604	1.57			
CE-123 3_03	4.515	9.306	2.676	1.62			
				Average	1.57	0.064	4.1
				Theory	1.81	0.50	27.6